

# Ultracold Feshbach Molecules

Francesca Ferlaino, Steven Knoop, and Rudolf Grimm  
*Institute of Experimental Physics and Center for Quantum Physics,  
 University of Innsbruck, 6020 Innsbruck, Austria, and  
 Institute for Quantum Optics and Quantum Information,  
 Austrian Academy of Sciences, 6020 Innsbruck, Austria*

## Contents

<b>I. Introduction</b>	1
A. Ultracold atoms and quantum gases	2
B. Basic physics of a Feshbach resonance	3
C. Binding energy regimes	5
<b>II. Making and detecting Feshbach molecules</b>	6
A. Bosons and fermions: role of quantum statistics	6
B. Overview of association methods	7
C. Purification schemes	9
D. Detection methods	9
<b>III. Internal-state manipulation near threshold</b>	10
A. Avoided level crossings	11
B. Cruising through the molecular spectrum	13
<b>IV. Halo dimers</b>	14
A. Halo dimers and universality	15
B. Collisional properties and few-body physics	16
C. Efimov three-body states	17
D. Molecular BEC	19
<b>V. Toward ground-state molecules</b>	20
A. Stimulated Raman adiabatic passage	21
B. STIRAP experiments	21
<b>VI. Further developments and concluding remarks</b>	24
<b>Acknowledgments</b>	25
<b>References</b>	25

## I. INTRODUCTION

The *coldest molecules* available for experiments are diatomic molecules produced by association techniques in ultracold atomic gases. The basic idea is to bind atoms together when they collide at extremely low kinetic energies. If any release of internal energy is avoided in this process, the molecular gas just inherits the ultralow temperature of the atomic gas, which can in practice be as low as a few nanokelvin.

If moreover a *single molecular quantum state* is selectively populated, there will be no increase of the system's entropy. A very efficient method to implement such a scenario in quantum-degenerate gases, Bose-Einstein condensates and Fermi gases, relies on the magnetically controlled association via Feshbach resonances. Such resonances serve as the entrance gate into the molecular world and allow for the conversion of atomic into molecular quantum gases.

In this Chapter, we give an introduction into experiments with *Feshbach molecules* and their various applications. Our illustrative examples are mainly based on work performed at Innsbruck University, but the reader will also find references to related work of other laboratories.

### A. Ultracold atoms and quantum gases

The development of techniques for cooling and trapping of atoms has lead to great advances in physics, which have already been recognized by two Nobel prizes. In 1997 the prize was jointly awarded to Steven Chu, Claude Cohen-Tannoudji and William D. Phillips “for their developments of methods to cool and trap atoms with laser light” [1, 2, 3]. In 2001, Eric A. Cornell, Wolfgang Ketterle and Carl E. Wieman jointly received the Nobel prize “for the achievement of Bose-Einstein condensation in dilute gases of alkali atoms, and for early fundamental studies of the properties of the condensates” [4, 5].

Laser cooling techniques allow researchers to prepare atoms in the microkelvin range. The key techniques have been developed since the early 80's and a detailed account can be found in Refs. [6, 7]. In brief, resonance radiation pressure is used to decelerate atoms from a thermal beam to velocities low enough to be captured into a so-called magneto-optical trap or, alternatively, low-velocity atoms can be captured into such a trap directly from a vapor. In the trap the atoms are further cooled by Doppler cooling to temperatures of the order of one millikelvin. Then, for some species, sub-Doppler cooling methods can be applied reducing the temperatures deep into the microkelvin range. Typical laser-cooled clouds contain up to about  $10^{10}$  atoms, and the atomic number densities are of the order of  $10^{11} \text{ cm}^{-3}$ . Such laser-cooled atoms have found numerous applications; a particularly important one is the realization of ultraprecise atomic clocks [8, 9].

The quantum-degenerate regime requires atomic de Broglie wavelengths to be similar to or larger than the interparticle spacing. As in laser-cooled clouds the phase-space densities are several orders of magnitude too low to reach this condition, further cooling needs to be applied. The method of choice is *evaporative cooling* [10], which can be applied in conservative traps like magnetic traps. Evaporative cooling relies on the selective removal of the most energetic atoms in combination with thermal equilibration of the sample by elastic collisions. The process can be forced by continuously lowering the trap depth. By trading one order of magnitude in the particle number one can gain up to typically three orders of magnitude in phase-space densities, and eventually reach the quantum-degenerate regime. The typical conditions are then a trapped gas of roughly a million atoms with densities of the order of  $10^{14} \text{ cm}^{-3}$  and temperatures in the nanokelvin range.

Quantum degeneracy has been achieved with bosonic and fermionic atoms. The attainment of Bose-Einstein condensation (BEC) in dilute ultracold gases marked the starting point of a new era in physics [11, 12, 13], and degenerate Fermi gases entered the stage a few years later [14, 15, 16]. The reader may be referred to the proceedings of the Varenna summer schools in 1998 and 2006 [17, 18], which describe these exciting developments. For reviews on the theory of degenerate quantum gases of bosons and fermions see [19] and [20], respectively, and the textbooks [21] and [22]. The trapping environment plays an important role for the applications of ultracold matter, including the present one to create molecules. Most of the experiments on molecule formation are performed with *optical dipole traps* [23] for two main reasons. Such optical traps can confine atoms in any Zeeman or hyperfine substate of the electronic ground state; this includes the particularly interesting lowest internal state, which cannot be

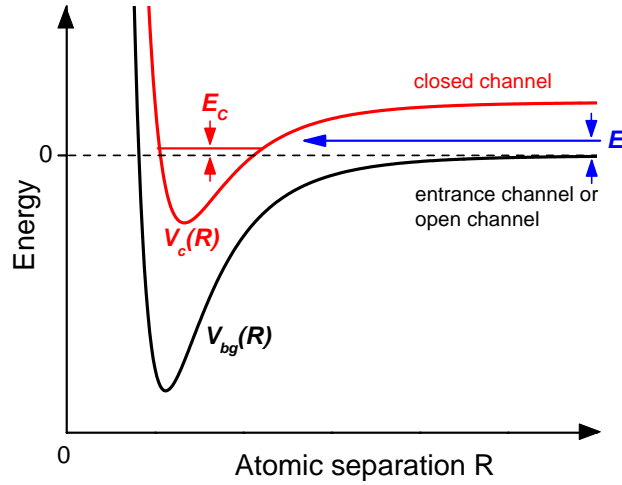


FIG. 1: Basic two-channel model for a Feshbach resonance. The phenomenon occurs when two atoms colliding at energy  $E$  in the entrance channel resonantly couple to a molecular bound state with energy  $E_c$  supported by the closed channel potential. In the ultracold domain, collisions take place near zero-energy,  $E \rightarrow 0$ . Resonant coupling is then conveniently realized by magnetically tuning  $E_c$  near 0 if the magnetic moments of the closed and open channel differ.

trapped magnetically. Moreover, optical dipole traps leave full freedom to apply any external magnetic fields, whereas in magnetic traps the application of additional magnetic fields would substantially affect the trapping geometry. A special optical trapping environment can be generated in *optical lattices* [24, 25]. Such lattices are created in optical standing-wave patterns, and in the three-dimensional case they provide an array of wavelength-sized microtraps, each of which may contain a single molecule.

The new field of ultracold molecular quantum gases rapidly emerged in 2002/03, when several groups reported on the formation of Feshbach molecules in BECs of  $^{85}\text{Rb}$  [26],  $^{133}\text{Cs}$  [27],  $^{87}\text{Rb}$  [28],  $^{23}\text{Na}$  [29], as well as in degenerate or near-degenerate Fermi gases of  $^{40}\text{K}$  [30] and  $^6\text{Li}$  [31, 32, 33]. Signatures of molecules in a BEC had been seen before using a photoassociative technique [34]. In the fall of 2003, the fast progress culminated in the creation of molecular Bose-Einstein condensates (mBEC) in atomic Fermi gases [35, 36, 37]. Heteronuclear Feshbach molecules entered the stage a few years later. So far, such molecules have been produced in Bose-Fermi mixtures of  $^{87}\text{Rb}$ - $^{40}\text{K}$  [38], and in Bose-Bose mixtures of  $^{85}\text{K}$ - $^{87}\text{Rb}$  [39] and  $^{41}\text{K}$ - $^{87}\text{Rb}$  [40]. The field of ultracold Feshbach molecules is developing rapidly, and there is great interest in homo- and heteronuclear molecules both in weakly bound and deeply bound regimes.

## B. Basic physics of a Feshbach resonance

Feshbach resonances represent the essential tool to control the interaction between the atoms in ultracold gases, which has been the key to many breakthroughs. Here we briefly outline the basic physics of a Feshbach resonance and its connection to the underlying near-threshold molecular structure. For more detailed discussions of the theoretical background see Chapters 6 and 11. The reader is also referred to two recent review articles [41, 42].

In a simple picture, we consider two molecular potential curves  $V_{bg}(R)$  and  $V_c(R)$ , as illustrated in Fig. 1. For large internuclear distances  $R$ , the background potential  $V_{bg}(R)$  asymptotically correlates with two free atoms in an ultracold gas. For a collision process with a very small energy  $E$ , this potential represents the energetically open channel, usually referred to as the *entrance channel*. The other potential,  $V_c(R)$ , representing the *closed channel*, is important as it can support bound molecular

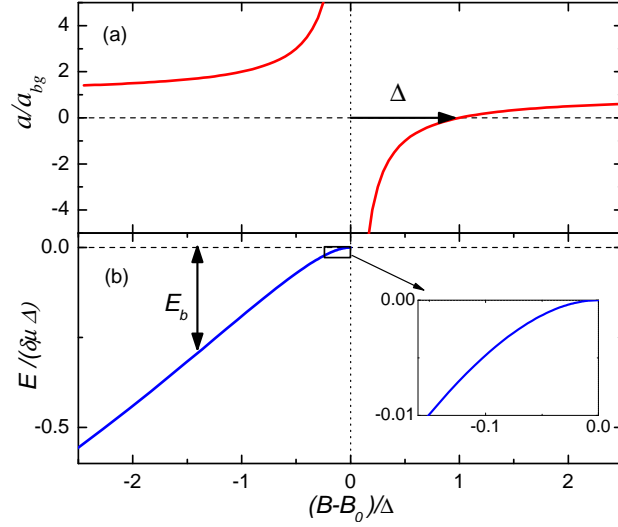


FIG. 2: Scattering length  $a$  (upper panel) and molecular state energy  $E$  (lower panel) near a magnetically tuned Feshbach resonance. The inset shows the universal regime near the point of resonance where  $a$  is very large and positive.

states near the threshold of the open channel.

A Feshbach resonance occurs when the bound molecular state in the closed channel is energetically close to the scattering state in the open channel, and some coupling leads to a mixing between the two channels. The energy difference can be controlled via a magnetic field when the corresponding magnetic moments are different. This leads to a *magnetically tunable Feshbach resonance*, which is the common way to achieve resonant coupling in the experiments with ultracold gases where the collision energy is practically zero.

A magnetically tuned Feshbach resonance can be described by a simple expression for the  $s$ -wave scattering length  $a$  as a function of the magnetic field  $B$ ,

$$a(B) = a_{\text{bg}} \left( 1 - \frac{\Delta}{B - B_0} \right). \quad (1)$$

Figure 2(a) illustrates this resonance expression. The *background scattering length*  $a_{\text{bg}}$ , which is the scattering length of  $V_{\text{bg}}(R)$ , represents the off-resonant value. It is directly related to the energy of the last bound vibrational level of  $V_{\text{bg}}(R)$ . The parameter  $B_0$  denotes the *resonance position*, where the scattering length diverges ( $a \rightarrow \pm\infty$ ), and the parameter  $\Delta$  is the *resonance width*.

The energy of the weakly bound molecular state near the resonance position  $B_0$  is shown in Fig. 2(b), relative to the threshold of two free atoms with zero kinetic energy. The energy approaches the threshold on the side of the resonance where  $a$  is large and positive. Away from the resonance, the energy varies linearly with  $B$  with a slope given by  $\delta\mu$ , the difference in magnetic moments of the open and closed channels. Near the resonance the coupling between the two channels mixes in entrance-channel contributions and strongly bends the molecular state.

In the vicinity of the resonance position at  $B_0$ , where the two channels are strongly coupled, the scattering length is very large. For large positive  $a$ , a “dressed” molecular state exists with a binding energy given by

$$E_{\text{b}} = \frac{\hbar^2}{2m_{\text{r}}a^2}, \quad (2)$$

where  $m_{\text{r}}$  is the reduced mass of the atom pair. In this limit,  $E_{\text{b}}$  depends quadratically on the magnetic detuning  $B - B_0$  and results in the bend depicted in the inset of Fig. 2. This region is of particular

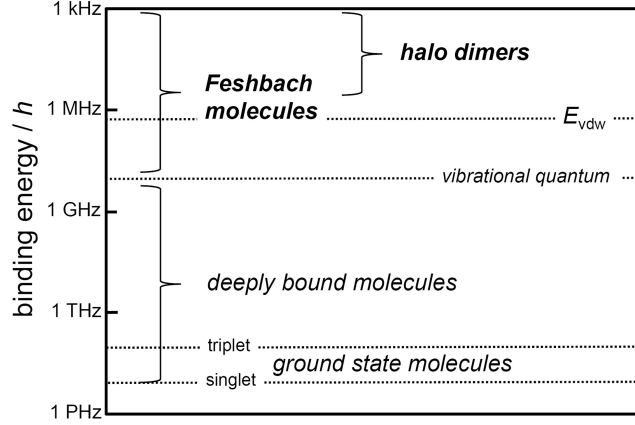


FIG. 3: Binding energy regimes for the example of  $\text{Cs}_2$  dimers, illustrated on a logarithmic scale. For the long-range van der Waals attraction between the atoms, a characteristic energy  $E_{\text{vdw}}$  is introduced; see Chapter 6 and Sec. IV. The vibrational quantum, here defined as the energy range below threshold in which one finds at least one bound state, corresponds to about  $40 E_{\text{vdw}}$ ; see Fig. 4 in Chapter 6. The binding energies of the vibrational ground state of the triplet and the single potential are typically five or six orders of magnitudes larger than this vibrational quantum.

interest because of its *universal* properties; see discussions in Chapters 6 and 11. Molecules formed in this regime are extremely weakly bound, and they are described by a wavefunction that extends far out of the classically allowed range. Such exotic molecules are therefore commonly referred to as *halo dimers*; we shall discuss their intriguing physics in Sec. IV.

These considerations show how a Feshbach resonance is inherently connected with a weakly bound molecular state. The key question for experimental applications is how to prepare the molecular state in a controlled way; we shall address this in Sec. II.

### C. Binding energy regimes

The name *Feshbach molecule* emphasizes the production method, as it commonly refers to diatomic molecules made in ultracold atomic gases via Feshbach resonances. But what are the physical properties associated with a Feshbach molecule, and what is the exact definition of such a molecule? It is quite obvious that a Feshbach molecule is a highly excited molecule, existing near the dissociation threshold and having an extremely small binding energy as compared to the one of the vibrational ground state. To give an exact definition, however, is hardly possible as the properties of molecules gradually change with increasing binding energy, and there is no distinct physical property associated with a Feshbach molecule. Molecules created via Feshbach resonances can be transferred to many other states near threshold (Sec. III) or to much more deeply bound states (Sec. V), thus being converted to more conventional molecules. There is no really meaningful definition of when a molecule can still be called a Feshbach molecule, or when it loses this character. We therefore use a loose definition and call a Feshbach molecule any molecule that exists near the threshold in the energy range set by roughly the quantum of vibrational energy. Any other molecule we consider a deeply bound molecule, although views may differ on this.

Figure 3 illustrates the vast range of molecular binding energies for the example of  $\text{Cs}_2$  dimers. According to our definition Feshbach molecules may have binding energies of up to roughly  $h \times 100 \text{ MHz}$  for the heavy  $\text{Cs}_2$  dimer and up to  $h \times 2.5 \text{ GHz}$  for the light  $\text{Li}_2$  dimer. These values are very small compared to the binding energies of ground state molecules, which are of the order of  $h \times 10 \text{ THz}$  or  $h \times 100 \text{ THz}$ .

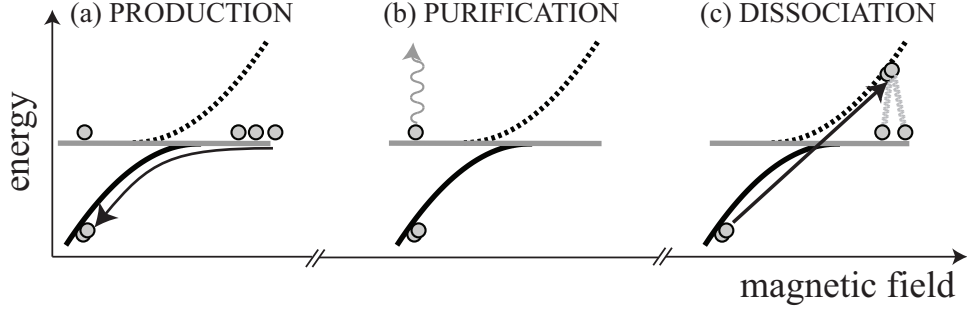


FIG. 4: Illustration of a typical experimental sequence to create, purify, and detect a sample of Feshbach molecules, (a) association via a magnetic-field sweep across the resonance, (b) selective removal of the remaining atoms, and (c) forced dissociation through a reverse magnetic field sweep. The dissociation is usually followed by imaging of the resulting cloud of atoms. The solid line corresponds to the bound molecular state, which intersects the threshold (gray horizontal line) and causes the Feshbach resonance; see also Fig. 2. The dashed line indicates the molecular state above threshold, where it has the character of a quasi-bound state coupling to the scattering continuum.

for the triplet and singlet potential, respectively. Nevertheless, ultracold Feshbach molecules can serve as the starting point for state transfer to produce very deeply bound, and even ground-state molecules, as we shall discuss in Sec. V.

Two particular regimes of Feshbach molecules can be realized close to the dissociation threshold. The *halo regime* requires binding energies well below the so-called van der Waals energy  $E_{\text{vdw}}$  (Sec. II in Chapter 6), which corresponds to about 3 MHz for  $\text{Cs}_2$  and about 600 MHz for  $\text{Li}_2$ . Molecules in high partial-wave states (Sec. III) can exist above the dissociation threshold, as the large centrifugal barrier prevents them from decaying; such *metastable Feshbach molecules* have a negative binding energy.

## II. MAKING AND DETECTING FESHBACH MOLECULES

This Section discusses how to create ultracold molecules, starting from a degenerate or near-degenerate atomic gas. The three main experimental steps are illustrated in Fig. 4. In a first step (a) atoms are converted into molecules, which can be done by sweeping the magnetic field across a Feshbach resonance. In a second step (b) a purification scheme can be applied that removes all the remaining atoms. In a third step (c) the molecules are forced to dissociate in a reverse sweep across the resonance in order to detect the resulting atoms. As an example, Figure 5 shows an image taken after the Stern-Gerlach separation of an atom-dimer mixture released from a trap; the smaller cloud represents a pure sample of Feshbach molecules. Similar techniques can also be applied to trapped atoms. In the following we describe the three steps of production, purification, and dissociation after a discussion of the important role of quantum statistics.

### A. Bosons and fermions: role of quantum statistics

Ultracold diatomic molecules can be composed either of two bosons, two fermions, or a boson and a fermion. In the first two cases, the molecules have bosonic character, while in the third case the molecules are fermions. Bosons are described by wavefunctions, which are symmetric with respect to exchange of identical particles, while, in the fermionic case, the wavefunctions are antisymmetric. This fundamental difference has important consequences.

Identical bosons (fermions) can collide in even (odd) partial waves. The role of partial waves is

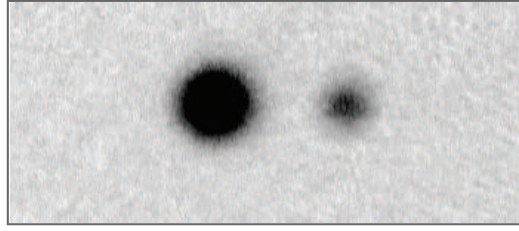


FIG. 5: Example for the preparation of a pure molecular cloud. Here an optically trapped BEC of  $^{87}\text{Rb}$  atoms was subjected to a magnetic-field sweep across a Feshbach resonance. The Stern-Gerlach technique was then applied after release from the trap to spatially separate the atoms (left) from the molecules (right). Finally the molecules were dissociated by a reverse Feshbach ramp, and an absorption image was taken. The field of view is  $1.7\text{ mm} \times 0.7\text{ mm}$ . Courtesy of S. Dür and G. Rempe.

discussed in Chapter 1. Here we use  $\ell$  as the corresponding angular momentum quantum number. The first partial-wave contribution for bosons (fermions) is then the  $s$ -wave with  $\ell = 0$  ( $p$ -wave with  $\ell = 1$ ) [43]. At ultralow temperatures, only  $s$ -wave collisions are dominant with the consequence that collisions between identical fermions are suppressed. The absence of  $s$ -wave collisions is also the reason why, for instance, direct evaporative cooling can not be applied to a sample of identical fermions. The situation changes when fermionic atoms are in different internal states, like hyperfine or Zeeman sublevels. The distinguishable particles can then interact in any partial wave. Fermion-composed molecules in  $s$ -wave states are therefore generally associated from ultracold two-component spin mixtures. Interactions in all partial waves are obviously allowed if two different atomic species are involved, regardless of their fermionic or bosonic character.

The quantum-statistical character of a molecule can crucially influence its collisional stability. Feshbach molecules in highly excited vibrational states are in principle very sensitive to vibrational relaxation induced by atom-molecule and molecule-molecule collisions. If such an inelastic relaxation process occurs, the energy release is very large as compared to the trap depth and will result in an immediate loss of all collision partners from the trap. A remarkable exception to this general behavior are Feshbach molecules composed of fermionic atoms in a halo state, as they exhibit an extremely high stability against inelastic decay. The reason of this different behavior is a Pauli suppression effect. In a two-component Fermi mixture, relaxation processes are unlikely since they necessarily involve at least two identical fermions; for more details see Chapter 10 and Ref. [44]. An intermediate case can be found for molecules composed in a Bose-Fermi mixture of two atomic species. Here, the collisional stability depends on the atomic partner involved in a collision, either a boson or a fermion. Only in collisions with fermionic atoms, a similar Pauli suppression effect can be expected.

The different degree of stability of bosons and fermions leads to a surprising result. One might think that the best way to achieve mBEC is the direct conversion of an atomic BEC. However, the stability of fermions turned out to be a key ingredient to experimentally achieve the condensation of molecules; see Sec. IV D. For attaining a collisionally stable mBEC of boson-composed molecules, their transfer into the rovibrational ground state (Sec. V) may be the only feasible way.

## B. Overview of association methods

The optimum association strategy depends on several factors connected to the specific system under investigation. The main factors to consider are the quantum-statistical nature of the atoms that form the molecule and the particular Feshbach resonance employed. Ultralow temperatures and high phase-space densities are essential requirements for an efficient molecule creation. Therefore all association



techniques start with an ultracold trapped atomic sample.

The most widespread technique for molecule association uses time-varying magnetic fields. The magnetic field modifies the energy difference between the scattering state and the molecular state. When the two states have the same energy, the scattering length diverges and a molecular state can be accessed in the region of positive scattering length ( $a > 0$ ); see Sec. IB.

Magnetic field time-sequences include linear ramps, fast jumps, or oscillating magnetic fields. Figure 4(a) illustrates a magnetic-field ramp, commonly referred to as “Feshbach ramp” [45, 46, 47]. A homogeneous magnetic field is swept across a Feshbach resonance from the side where  $a < 0$  to the side where  $a > 0$ . The coupling between atom pairs and molecules removes the degeneracy at the crossing of the two corresponding energy levels. The resulting avoided level crossing can be used to adiabatically convert atom pairs into molecules by sweeping the magnetic field across the resonance, as indicated by the arrow in Fig. 4(a). The atomic sample is partially converted into a molecular gas. In the fermionic case, the conversion efficiency does solely depend on the ramp speed and on the atomic phase-space density [48], and can reach values close to one. In the case of bosons, the conversion efficiency is affected by inelastic collision processes. Near the center of a Feshbach resonance, the atoms experience a huge increase of the three-body recombination rate, while, after the association, the atom-dimer mixture can undergo fast collisional relaxation. The best parameters for molecule association require a compromise for the optimum ramp speed, which should be slow enough for an efficient conversion, but fast enough to avoid detrimental losses.

Inelastic collisional loss can be reduced by using more elaborate time sequences for the magnetic field or, alternatively, resonant radio-frequency techniques. The key idea is to introduce an efficient atom-molecule coupling while minimizing the time spent near the resonance, where strong loss and heating results from inelastic interactions. An efficient technique is to apply a small sinusoidal modulation to the homogeneous field. The oscillating field then induces a corresponding modulation of the energy difference between the scattering state and the molecular state. The molecules are associated when the modulation frequencies match the molecular binding energies [49]. Typical modulation frequencies range from a few kHz to a few 100 kHz. The signature of molecule production is a resonant decrease of the atom number, as observed in gases of  $^{85}\text{Rb}$  [50] and  $^{40}\text{K}$  [51], and in a mixture of the two isotopes  $^{85}\text{Rb}$  and  $^{87}\text{Rb}$  [39]. A resonant coupling between atom pairs and molecules can also be induced by a radio-frequency excitation, which stimulates a transition between the atom pair state and the molecular state without modulating the energy difference. Heteronuclear  $^{40}\text{K}^{87}\text{Rb}$  molecules were produced with this technique both in an optical lattice [38] and in an optical dipole trap [52].

Collisional losses can also be suppressed by using a suitable trapping environment. This is the case when atoms are prepared in an optical lattice with double site occupancy. A stable system with a single molecule in each lattice site can then be created using, for instance, a Feshbach ramp [53, 54].

A completely different association strategy can be applied to create molecules in an atomic Fermi gas of  $^6\text{Li}$  atoms. This special situation is particularly important as it has opened up a simple and efficient route towards mBEC [36, 37]; see also Sec. IVD. Near a Feshbach resonance, in the regime of very large positive scattering lengths, atomic *three-body recombination* efficiently produces halo dimers. In a three-body recombination event in a two-component atomic Fermi gas, two non-identical fermions bind into a molecule while the third atom carries away the leftover energy and momentum. Usually, the energy released in three-body collisions is very large so that all collision partners immediately leave the trap. However, for the special case of halo dimers, the very small binding energies can be on the order of the typical thermal energies of the trapped particles and thus less than the trap depth [18]. The formation of halo dimers via three-body recombination then proceeds with small heating and negligible trap losses. This way of forming molecules can also be interpreted in terms of a thermal atom-molecule equilibrium [55, 56]. Typical time scales for the atom-molecule thermalization are on the order of 100 ms to 1 s, requiring the high collisional stability of fermion-composed molecules in the halo regime. As an



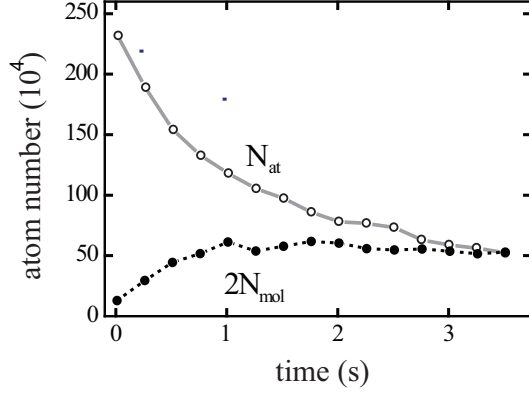


FIG. 6: Formation of  ${}^6\text{Li}_2$  halo dimers via three-body recombination. The molecules are created in an optically trapped spin mixture of atomic  ${}^6\text{Li}$  at a temperature of  $3\,\mu\text{K}$ . The experiment is performed near a broad Feshbach resonance, where  $a = +1420a_0$  and  $E_b = k_B \times 15\,\mu\text{K} = h \times 310\,\text{kHz}$ .  $N_{\text{at}}$  and  $N_{\text{mol}}$  denote the number of unbound atoms and the number of molecules, respectively. Adapted from Ref. [32].

example, Fig. 6 shows how an initially pure sample of  ${}^6\text{Li}$  atoms changes into an atom-molecule mixture [32].

### C. Purification schemes

Purification is an important step in many experiments with Feshbach molecules. The removal of atoms can be needed to avoid fast collisional losses of molecules. In other cases, pure molecular samples are needed for particular applications. Most of the purification schemes act selectively on atoms and they are applied on time scales short compared to the typical molecular lifetimes.

A possible purification strategy exploits the difference in magnetic moments of molecules and atoms. The two components of the gas can be spatially separated with the Stern-Gerlach technique, which uses magnetic field gradients [27, 28]; for an example see Fig. 5. This method is usually applied to gases in free space after release from the trap.

A fast and efficient purification method, well suited for the application to a trapped cloud, uses resonant light to push the atoms out of the sample by resonant radiation pressure [29, 53, 57]. The “blast” light needs to be resonant with a cycling atomic transition, which allows for the repeated scattering of photons. In many cases, the atoms are not in a ground-state sublevel connected to a cycling optical transition, so that an intermediate step is necessary. In the most simple implementation, this is an optical pumping step that selectively acts on the atoms without affecting the molecules. Alternatively a microwave pulse can be used to transfer the atoms into the appropriate atomic level. The high selectivity of this double-resonance method minimizes residual heating and losses of molecules from the trap.

### D. Detection methods

A very efficient way to detect Feshbach molecules is to convert them back into atom pairs and to take an image of the reconverted atoms with standard absorption imaging techniques [27, 28]. In principle, each of the above-described association methods can be reverted and turned into a corresponding dissociation scheme.

A robust and commonly used dissociation scheme is to simply reverse the Feshbach ramp, as illustrated in Fig. 4(c). The reverted ramp is usually chosen to be much faster than the one employed for association.

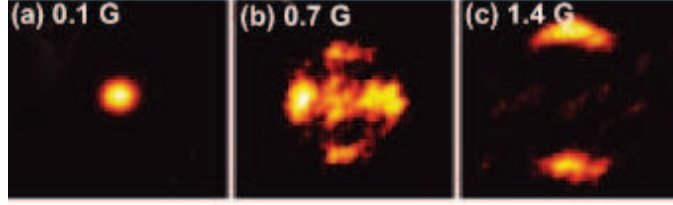


FIG. 7: Dissociation patterns of  $^{87}\text{Rb}_2$  molecules near a  $d$ -wave shape resonance. The molecules can dissociate either directly into the continuum or indirectly by passing through a  $d$ -wave shape-resonance state located behind the centrifugal barrier. Initially, the direct dissociation process dominates and preferentially populates isotropic  $s$ -wave states (a). Approaching the shape resonance, the pattern reveals first an interference between  $s$ - and  $d$ -partial waves (b), and then shows a pure outgoing  $d$ -wave (c). The given magnetic field values are relative to the field where dissociation is observed to set in. Adapted from Ref. [58].

The molecules are then brought into a quasi-bound state above the atomic threshold. Here they quickly dissociate into atom pairs, converting the dissociation energy into kinetic energy. The back-ramp is usually done in free space and can be performed either immediately after release from the trap or after some expansion time ( $\approx 10 - 30$  ms). The choice of the delay time between the dissociation and the detection sets the type of information that can be extracted from the absorption image. For a long delay time, the sample expands thus mapping the information on the momentum distribution onto the spatial distribution. The image then contains quantitative information on the dissociation energy [59]. For a short delay time, the absorption image simply reflects the spatial distribution of the molecules before the dissociation.

Fast and efficient dissociation requires a sufficiently strong coupling of the molecular states to the scattering continuum. Molecular states with high rotational quantum number  $\ell$  typically have weak couplings and high centrifugal barriers. A striking example is provided by  $\text{Cs}_2$  Feshbach molecules with  $\ell = 8$  [43]. These molecules do not sufficiently couple to the atomic continuum and dissociation is prevented. There are two ways to detect them. The first is based on a time reversal of the association path (Sec. III B) [60]. The second exploits the crossing and the mixing with a quasi-bound state above threshold with  $\ell \leq 4$  to force the dissociation [61].

Dissociation patterns can also provide additional spectroscopic information. An example is shown in Fig. 7. Here the dissociation patterns of  $^{87}\text{Rb}_2$  show strong modifications by the presence of a  $d$ -wave shape resonance [58].

In the halo regime, molecules can be detected by direct imaging [37, 62]. The imaging frequency for halo molecules is very close to the atomic frequency. Presumably, the first photon dissociates the molecule into two atoms, which then absorb the subsequent photons. In the case of heteronuclear molecules, directed imaging is possible in a wider range of binding energies. This happens because the excited and ground molecular potentials both vary as  $1/R^6$ ; see Chapter 5. In the homonuclear case, the excited potential varies as  $1/R^3$  [63].

### III. INTERNAL-STATE MANIPULATION NEAR THRESHOLD

Below the atomic threshold a manifold of molecular states exists. They correspond to different vibrational, rotational and magnetic quantum numbers, and belong to potentials correlated with different hyperfine states. Having different magnetic moments, many levels cross when the magnetic field is varied. When some coupling between two molecular states that cross is present an avoided crossing occurs. The concept of avoided level crossings is very general and has found important applications in many fields of physics. We have already discussed the application to associate molecules in Sec. II.

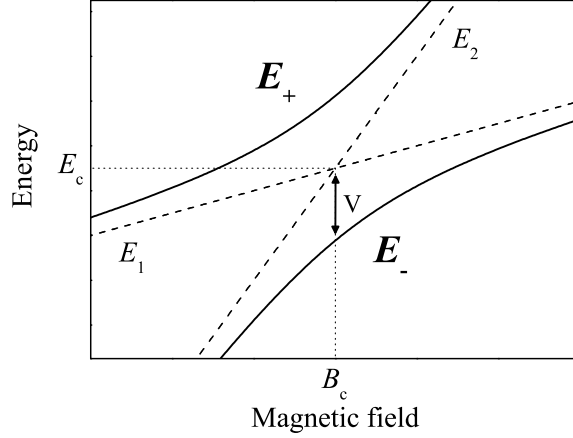


FIG. 8: Schematic representation of an avoided crossing between two molecular states. The dashed lines represent the diabatic states with energies  $E_1$  and  $E_2$ , with a crossing at  $B_c$ . The solid lines represent the adiabatic states with energies  $E_+$  and  $E_-$ , caused by a coupling  $V$  between the two diabatic states.

In the field of ultracold molecules, the information on the avoided crossings is fundamentally important to fully describe the molecular spectrum and to understand the coupling mechanisms between different states. At the same time controlled state transfer near avoided crossings opens up the intriguing possibility to populate many different molecular states that are not directly accessible by Feshbach association.

#### A. Avoided level crossings

If an avoided crossing is well separated from any other avoided crossing, including the one resulting near threshold from the coupling to the scattering continuum, a simple two-state model can be applied. Consider two molecular states ( $i = 1, 2$ ), for which the magnetic field dependencies of the binding energies  $E_i$  of the diabatic states  $\varphi_i$  are given by

$$E_i(B) = \mu_i(B - B_c) + E_c, \quad (3)$$

where  $\mu_i$  are the magnetic moments, and  $B_c$  and  $E_c$ , the magnetic field and energy at which the two states cross, respectively; see Fig. 8. The crossing is conveniently described in terms of adiabatic states if the two states are coupled by the interaction Hamiltonian  $H$ , i.e.  $\langle \varphi_1 | H | \varphi_2 \rangle \neq 0$ . To obtain the corresponding adiabatic energies one has to solve the following eigenvalue problem,

$$\begin{pmatrix} E_1 & V \\ V & E_2 \end{pmatrix} \begin{pmatrix} \varphi_1 \\ \varphi_2 \end{pmatrix} = E \begin{pmatrix} \varphi_1 \\ \varphi_2 \end{pmatrix},$$

where  $V = \langle \varphi_1 | H | \varphi_2 \rangle$  is the coupling strength between the diabatic states. The adiabatic energies are given by

$$2E_{\pm} = (E_1 + E_2) \pm \sqrt{(E_1 - E_2)^2 + 4V^2}, \quad (4)$$

where the energies  $E_+$  and  $E_-$  correspond to the upper and lower adiabatic levels of the avoided crossing. The energy difference between the adiabatic levels is

$$\Delta E = |E_+ - E_-| = \sqrt{(\mu_1 - \mu_2)^2(B - B_c)^2 + 4V^2}, \quad (5)$$

which at the crossing is twice the coupling strength, i.e.  $\Delta E(B_c) = 2V$ .

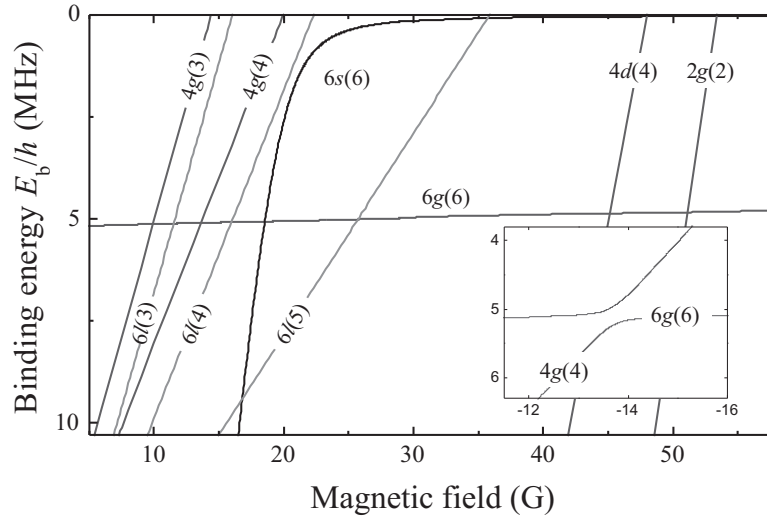


FIG. 9: Molecular energy structure of  $\text{Cs}_2$  below the threshold of two free Cs atoms in the absolute hyperfine ground-state sublevel. The molecular states near threshold are well characterized by quantum numbers  $|f, m_f; \ell, m_\ell\rangle$  [41], where  $f$  represents the sum of the total atomic spins  $F_{1,2}$  of the individual atoms, and  $\ell$  is the rotational quantum number. The respective projection quantum numbers are given by  $m_f$  and  $m_\ell$ . The interaction Hamiltonian conserves  $f + \ell$  at zero magnetic field, and always conserves  $m_f + m_\ell$ . In this example, Feshbach association is performed with pair of atoms that has  $m_f + m_\ell = 6$ , and only molecular states with  $m_f + m_\ell = 6$  have to be considered. Therefore the labeling  $f\ell(m_f)$  is sufficient to characterize the molecular states. Due to relatively strong relativistic spin-spin dipole and second-order spin-orbit interactions, molecular states with rotational quantum number up to  $l$ -wave ( $\ell = 8$ ) have to be taken into account in the case of Cs. The inset shows one of the narrow avoided crossings between two molecular states. Adapted from Ref. [57].

Let us illustrate the occurrence of avoided level crossings by the example of  $\text{Cs}_2$ , for which the near-threshold spectrum is shown in Fig. 9. The molecular spectrum of  $\text{Cs}_2$  provides many avoided crossings, basically for two reasons. First of all, there exists a high density of molecular levels because its large mass gives rise to a small vibrational and rotation spacing, and its large nuclear spin gives rise to many hyperfine substates. Secondly, relatively strong relativistic spin-spin dipole and second-order spin-orbit interactions couple many of these states. Most crossings in Fig. 9 are indeed avoided crossings and the inset shows one in an expanded view as an example. As they are well separated from each other, the simple two-state model applies very well.

The crossing position  $B_c$  and the coupling strength  $V$  can be measured by different methods. Magnetic moment spectroscopy relies on measuring the effect of a magnetic field gradient after the molecular cloud is released from the trap. The difference in the position of a molecular cloud after a fixed time-of-flight with and without a magnetic field gradient is directly proportional to the magnetic moment. In the avoided crossing region the magnetic moment of the adiabatic molecular states shows a rapid change with magnetic field. This technique has been applied to map out several avoided crossings of the  $\text{Cs}_2$  spectrum, from which one is shown in Fig. 10(a). Another method relies on direct probing of  $\Delta E$  by radio-frequency excitation between the adiabatic states, as demonstrated for  $^{87}\text{Rb}_2$  [64].

More sophisticated methods rely on Ramsey-type or Stückelberg interferometry, which have been applied to avoided crossings in  $^{87}\text{Rb}_2$  [64] and  $\text{Cs}_2$  [60], respectively. In the Ramsey scheme a radio-frequency pulse creates a coherent superposition. After a hold time and a second pulse, the population in one of the molecular branches is measured. This population shows an oscillation as function of the hold time with a frequency of  $\Delta E/h$ . In the Stückelberg scheme a coherent superposition is obtained by a magnetic field sweep over the avoided crossing; see Sec. III B. After a hold time, a reverse magnetic field sweep is applied and the population in both molecular branches is measured. Here the oscillation

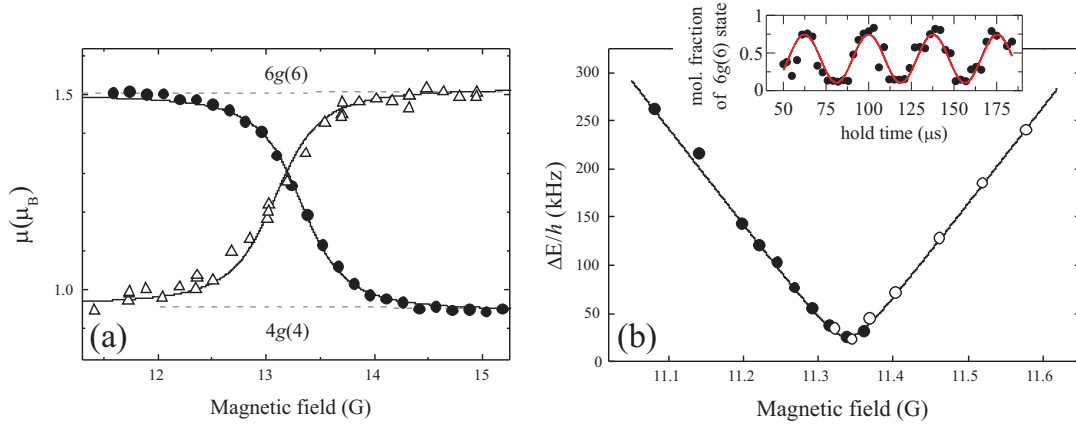


FIG. 10: Examples of two different techniques to map avoided crossings, both applied to  $\text{Cs}_2$ . (a) Magnetic moment spectroscopy on the two molecular states around the  $6g(6)/4g(4)$  avoided crossing, measuring the magnetic moment as function of the magnetic field. A fit to the data gives  $B_c=13.29(4)$  G and  $V = h \times 164(30)$  kHz. (b) Stückelberg interferometry on the two molecular states around the  $6g(6)/6l(3)$  avoided crossing. The solid curve is a fit according to Eq. 5, resulting in  $B_c=11.339(1)$  G and  $V = h \times 14(1)$  kHz. Inset: raw data showing an oscillation of the population in state  $6g(6)$  right in the center of the crossing. Panel (a) adapted from Ref. [57], panel (b) from Ref. [60].

frequency in the population is also equal to  $\Delta E/h$ . In Fig. 10(b) the mapping of a very narrow avoided crossing with the Stückelberg scheme is shown.

### B. Cruising through the molecular spectrum

A magnetic field ramp over the avoided crossing can be used for state-transfer. When the magnetic field is ramped slowly, the population follows the adiabatic states. This is called an adiabatic ramp. If the change in magnetic field is very fast, the molecules do not experience the coupling between the diabatic states, and therefore remain in their initial state. This is a non-adiabatic ramp. The well-known Landau-Zener model describes the final population in both molecular states after the ramp. The probability of adiabatic transfer is given by

$$p = 1 - \exp\left(-\dot{B}_c/|\dot{B}|\right), \quad (6)$$

where  $\dot{B}$  is the linear ramp speed and  $\dot{B}_c = 2\pi V^2/(\hbar|\mu_1 - \mu_2|)$ . An adiabatic ramp corresponds to a ramp speed of  $|\dot{B}| \ll \dot{B}_c$ , while a non-adiabatic ramp requires  $|\dot{B}| \gg \dot{B}_c$ .

Manipulation of the population over avoided crossings is fully coherent as there is no dissipation. Intermediate ramp speeds result in a coherent splitting of the population over the two molecular states. This property was demonstrated by a Stückelberg interferometer, in which two subsequent passages through an avoided crossing in combination with a variable hold time lead to high-contrast population oscillations, as shown in the inset of Fig. 10(b). The required ramp speed for equal splitting is on the order of  $1 \text{ G}/\mu\text{s}$  for an avoided crossing with  $V \sim h \times 100$  kHz.

The magnetic field ramps over avoided crossings allow to populate states that are not directly accessible by Feshbach association. This includes states that do not cross the atomic threshold, for example the  $6g(6)$  state in Fig. 9. There are also states that do cross the atomic threshold, but do not induce Feshbach resonances as the coupling with the atomic continuum is too weak. This occurs for molecular states with high rotational quantum number. For  $\text{Cs}_2$  molecular states with  $\ell > 4$ , e.g. the  $l$ -wave states shown in Fig. 9, no Feshbach resonances exist. In Refs. [57, 61] the population of the  $l$ -wave states using avoided

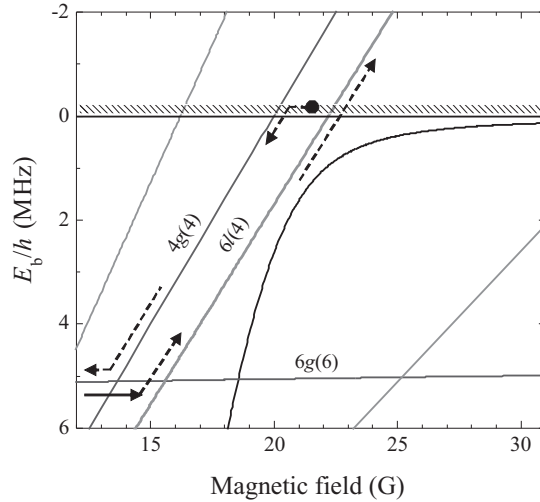


FIG. 11: Population scheme for the  $\text{Cs}_2$   $6l(4)$  state. Starting with Feshbach association on the 19.8-G  $g$ -wave Feshbach resonance, the resulting  $4g(4)$  Feshbach molecules are brought to larger binding energies by ramping down the magnetic field. At a binding energy of about  $h \times 5$  MHz, the avoided crossing with the  $6g(6)$  state is followed adiabatically. Then a fast ramp in the opposite direction is made, jumping the avoided crossing, after which a slow magnetic field ramp towards higher magnetic fields leads to adiabatic transfer from the  $6g(6)$  to the  $6l(4)$  state. The molecular sample in the  $6l(4)$  state can be brought above the atomic threshold, as the large centrifugal barrier prohibits dissociation. Adapted from Ref. [61].

crossings was demonstrated. As an example, the population scheme for one of the  $l$ -wave states is shown in Fig. 11.

The ability to populate molecular states that do not induce Feshbach resonances raises the question on the lifetime of these states above the atomic threshold, as the vanishing coupling with the atomic continuum implies that dissociation is suppressed. By studying the lifetime of the molecular sample above threshold it was found that  $l$ -wave molecules are indeed stable against dissociation on a timescale of 1 s [61]. The preparation of long-lived Feshbach molecules above the atomic threshold opens up the possibility to create novel metastable quantum states with strong pair correlations.

The method of jumping avoided crossings is in practice limited to crossings with energy splittings up to typically  $h \times 200$  kHz. For stronger crossings, fast ramps are technically impracticable and the crossings are followed adiabatically when the magnetic field is ramped, leaving no choice for the state transfer. This problem can be overcome with the help of radio-frequency excitation [64]. For  $^{87}\text{Rb}_2$  the transfer of molecules over nine level crossings was demonstrated when the magnetic field was ramped down from a Feshbach resonance near 1 kG to zero. This efficiently produced molecules with a binding energy  $E_b = h \times 3.6$  GHz at zero magnetic field. The combination of these elaborate ramp and radio-frequency techniques allows for cruising through the complex molecular energy structure. The level spectrum serves as a molecular “street map” and by passing straight through crossings or performing left or right turns one can reach any desired destination.

#### IV. HALO DIMERS

Very close to resonance the Feshbach molecules are extremely weakly bound and become *halo dimers*. This halo regime is interesting because of its universal properties, regarding its intrinsic behavior (Sec. IV A) and its few-body interaction properties (Sec. IV B), in particular in the context of Efimov physics (Sec. IV C). The properties of fermion-composed halo dimers, extensively discussed in

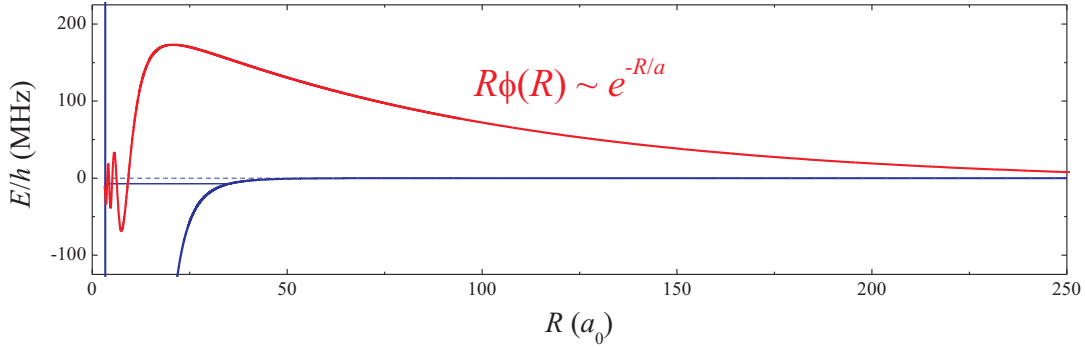


FIG. 12: Radial wavefunction of a halo dimer, where  $R$  is the interatomic distance, extending far into the classically forbidden range where the wavefunction is proportional to  $e^{-R/a}$ . The wavefunction is calculated for a Lennard-Jones potential and  $m_r = 3$  a.m.u. [65]. The potential depth is tuned such that the highest vibrational level, in this case  $v = 5$ , is in the halo regime.

Chapter 10, allow the realization of molecular Bose-Einstein condensation (mBEC), which is the topic of Sec. IV D.

### A. Halo dimers and universality

For large scattering lengths  $a$ , the Feshbach molecule enters the halo regime, where its binding energy is given by Eq. 2. Its magnetic field dependence is illustrated in the inset of Fig. 2. The halo state can be described in terms of a single effective molecular potential having scattering length  $a$ . In Fig. 12 a typical halo wavefunction is shown as function of the interatomic distance  $R$ . This highlights its remarkable property to extend far into the classically forbidden range, which is at the heart of its universal properties. The asymptotic form of the halo wavefunction is proportional to  $e^{-R/a}$  and the average distance between the two atoms is  $a/2$ ; see also Sec. V of Chapter 11.

The halo regime requires  $a$  to be much larger than the range of the two-body potential. For ground state alkali atoms a characteristic range can be described by the van der Waals length  $R_{\text{vdw}} = \frac{1}{2}(2m_r C_6/\hbar^2)^{1/4}$ , where  $C_6$  is the van der Waals dispersion coefficient; see Chapter 6 and 10. The corresponding van der Waals energy is  $E_{\text{vdw}} = \hbar^2/(2m_r R_{\text{vdw}}^2)$ . Thus a halo dimer can be defined through the criteria  $a \gg R_{\text{vdw}}$  and  $E_b \ll E_{\text{vdw}}$ . For some examples the van der Waals scales are given in Table I, where  $R_{\text{vdw}}$  is expressed in units of the Bohr radius  $a_0 = 0.529 \times 10^{-10}$  m.

The halo regime corresponds to the *universal regime* for  $a > 0$ . The concept of universality is that the properties of any physical system in which  $|a|$  is much larger than the range of the interaction is determined by  $a$ , and therefore all these systems exhibit the same *universal* behavior [66]. In the universal regime the details of the short range interaction become irrelevant because of the dominant long-range nature of the wavefunction. The existence of the halo dimer at large positive  $a$  is a manifestation of universality in two-body physics [67]. Halo states are known in nuclear physics, with the deuteron being a prominent example. In molecular physics, the He dimer has for many years served as the prime example of a halo state. Feshbach molecules with halo character are special to other halo states in the sense that their properties are magnetically tunable. In particular, one can scan from the universal regime of halo dimers to the non-universal regime of non-halo Feshbach molecules.

In principle, every Feshbach resonance features a halo region. In practice, however, only a few resonances are suited to experimentally realize this interesting regime. Those are broad resonances with large widths  $|\Delta|$  (typically  $\gg 1$  G) and large background scattering lengths  $|a_{\text{bg}}|$  that exceed  $R_{\text{vdw}}$  [41, 42]. Prominent examples are found in the two fermionic systems  $^6\text{Li}$  and  $^{40}\text{K}$ , and the bosonic systems  $^{39}\text{K}$ ,



TABLE I: Characteristic van der Waals scales  $R_{\text{vdw}}$  and  $E_{\text{vdw}}$  for some selected examples.

	$^6\text{Li}_2$	$^{40}\text{K}_2$	$^{40}\text{K}^{87}\text{Rb}$	$^{85}\text{Rb}_2$	$^{133}\text{Cs}_2$
$R_{\text{vdw}} (a_0)$	31	65	72	82	101
$E_{\text{vdw}}/h$ (MHz)	614	21	13	6.2	2.7

$^{85}\text{Rb}$  and  $^{133}\text{Cs}$ , some of which are discussed in Sec. IV of Chapter 6 and Sec. V of Chapter 11.

Another universal feature of a halo dimer regards spontaneous dissociation, which is possible when its atomic constituents are not in the lowest internal states and open decay channels are present. In the halo regime the dissociation rate scales as  $a^{-3}$ , as has been observed for  $^{85}\text{Rb}_2$  [68], and can be understood as a direct consequence of the large halo wavefunction [69].

### B. Collisional properties and few-body physics

The concept of universality extends beyond two-body physics to few-body phenomena, including the low-energy scattering properties of halo dimers. The *inelastic* collisional properties are important as inelastic collisions usually lead to trap loss, determining the lifetime of a sample of trapped halo dimers. At the same they provide a convenient experimental observable to study few-body physics. In general, the loss of dimers can be described by the following rate equation:

$$\dot{n}_{\text{D}} = -\alpha n_{\text{D}}^2 - \beta n_{\text{D}} n_{\text{A}}, \quad (7)$$

where  $\alpha$  and  $\beta$  are the loss rate coefficients for dimer-dimer and atom-dimer collisions, respectively, and  $n_{\text{A}}(n_{\text{D}})$  is the atomic (molecular) density. Fast trap loss has been observed for Feshbach molecules in the non-universal regime, with  $\alpha$  and  $\beta$  on the order of  $10^{-11}$ - $10^{-10}$   $\text{cm}^3\text{s}^{-1}$ ; see Sec. III of Chapter 3. The loss coefficient  $\alpha$  is most conveniently measured using a pure molecular sample. To determine  $\beta$  an atom-dimer mixture is required, the atom number greatly exceeding the molecule number being beneficial.

In the universal regime, simple scaling laws for  $\alpha$  and  $\beta$  can be derived. For halo dimers composed of two identical bosons  $\beta$  scales linearly with  $a$  [70, 71], resulting in an enhancement of dimer loss near a Feshbach resonance. In contrast, for halo dimers made of two fermions in different spin states an  $a^{-2.55}$  and an  $a^{-3.33}$  scaling are derived for  $\alpha$  and  $\beta$  [44], respectively, connected to the collisional stability of the molecular sample near a Feshbach resonance, as discussed in Sec. II A. Universal scaling laws are also derived for other atom-dimer systems [52, 72], as well as for the related problem of three-body recombination in atomic samples [71, 72].

Inelastic dimer-dimer scattering represents an elementary four-body process. For four identical bosons a universal prediction has so far not been derived, as the four-body problem is substantially more challenging than the three-body problem. Experimentally one can investigate this process by measuring  $\alpha$  in a pure molecular sample of halo dimers made of identical bosons, which has been done in the case of  $\text{Cs}_2$  [73]. The results are given in Fig. 13, showing a strong scattering length dependence of  $\alpha$ . A pronounced loss minimum around  $500a_0$  is observed, followed by a linear increase towards larger  $a$ . The interpretation of this striking behavior is still an open issue and might stimulate progress in the theoretical description of the four-body problem.

For the *elastic* scattering properties, universal scaling laws have been derived for fermion-composed halo dimers. Both the atom-dimer and dimer-dimer scattering lengths simply scale with the atom-atom scattering length  $a$ , namely as  $1.2a$  [74] and  $0.6a$  [44], respectively. Therefore the elastic cross sections, being proportional to the square of these scattering lengths, are very large in the halo region. This leads to fast thermalization in an atom-dimer mixture and a pure dimer sample, opening the possibility of

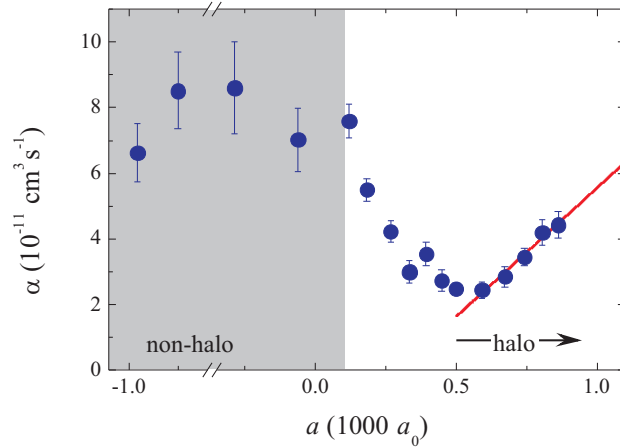


FIG. 13: Experimental study of the interaction between halo dimers. The relaxation rate coefficient  $\alpha$  for inelastic dimer-dimer scattering is measured as function of the scattering length  $a$  for a pure sample of optically trapped Cs Feshbach molecules. The experiment makes use of the wide tunability of the scattering length for Cs, in particular into the halo regime. The solid line is a linear fit to the data in the region  $a \geq 500 a_0$ . The shaded region indicates the  $a < R_{\text{vdw}}$  regime, where the Feshbach molecules are not in a halo state. Adapted from Ref. [73].

evaporative cooling. For boson-composed halo dimers the few-body problem is more complicated and universal predictions for their elastic scattering properties are so far lacking.

### C. Efimov three-body states

Efimov quantum states in a system of three identical bosons [75, 76] are a paradigm for universal few-body physics. These states have attracted considerable interest, fueled by their bizarre and counter-intuitive properties and by the fact that they had been elusive to experimentalists for more than 35 years. In 2006, experimental evidence for Efimov states in an ultracold gas of Cs atoms was reported [77]. In the context of ultracold quantum gases, Efimov physics manifests itself in three-body decay properties, such as resonances in the three-body recombination and atom-dimer relaxation loss rates. These resonances appear on top of the non-resonant “background” scattering behavior, given by the universal scaling laws discussed in Sec. IV B.

Efimov’s scenario is illustrated in Fig. 14, showing the energy spectrum of the three-body system as a function of the inverse scattering length  $1/a$ . For  $a < 0$ , the natural three-body dissociation threshold is at zero energy. States below are trimer states and states above are continuum states of three free atoms. For  $a > 0$ , the dissociation threshold is given by the binding energy of the halo dimer; at this threshold a trimer dissociates into a halo dimer and an atom. Efimov predicted an infinite series of weakly bound trimer states with universal scaling behavior. When the scattering length is increased by a universal scaling factor  $e^{\pi/s_0}$ , a new Efimov state appears, which is just larger by this factor and has a weaker binding energy by a factor  $e^{2\pi/s_0}$ . For three identical bosons  $s_0 \approx 1.00624$ , so that the scaling factors for the scattering length and the binding energy are 22.7 and  $22.7^2 \approx 515$ , respectively. For  $a < 0$ , Efimov states are “Borromean” states [67], which means that a weakly bound three-body state exists in the absence of a weakly bound two-body state. This property that three quantum objects stay together without pairwise binding is part of the bizarre nature of Efimov states.

The Efimov trimers influence the three-body scattering properties. When an Efimov state intersects the continuum threshold for  $a < 0$  three-body recombination loss is enhanced [79, 80], as the resonant coupling of three atoms to an Efimov state opens up fast decay channels into deeply bound dimer states

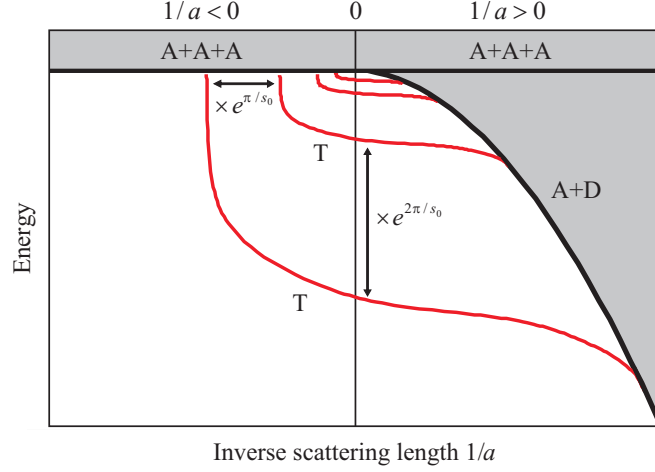


FIG. 14: Efimov's scenario. Appearance of an infinite series of weakly bound Efimov trimer states (T) for resonant two-body interaction, showing a logarithmic-periodic pattern with universal scaling factors  $e^{\pi/s_0}$  and  $e^{2\pi/s_0}$  for the scattering length and the binding energy, respectively. The binding energy is plotted as a function of the inverse two-body scattering length  $1/a$ . The gray regions indicate the scattering continuum for three atoms (A+A+A) and for an atom and a halo dimer (A+D). To illustrate the series of Efimov states, the universal scaling factor is artificially set to 2.

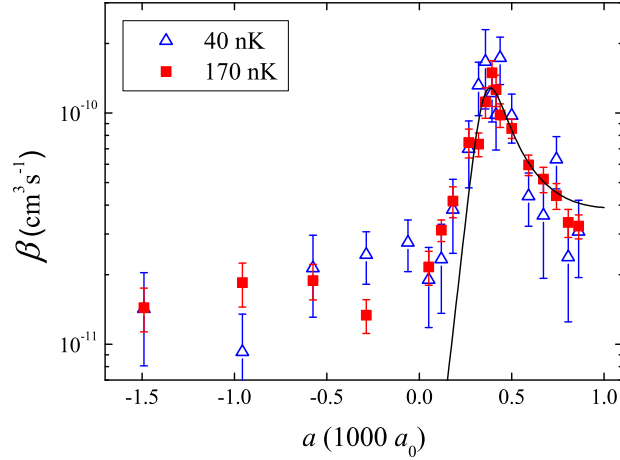


FIG. 15: Observation of a scattering resonance in an ultracold, optically trapped mixture of Cs atoms and  $\text{Cs}_2$  halo dimers. As for Fig. 13, one benefits from the wide tunability of the scattering length provided by Cs. The data show the loss rate coefficient for atom-dimer relaxation  $\beta$  for temperatures of 40(10) nK and 170(20) nK. A pronounced resonance is observed at about  $+400 a_0$ , corresponding to a magnetic field of 25 G. The solid curve is a fit of an analytic model from effective field theory [66] to the data for  $a > R_{\text{vdw}}$ . Adapted from Ref. [78].

plus a free atom. Such an Efimov resonance has been observed in an ultracold, thermal gas of Cs atoms [77]. For  $a > 0$  a similar phenomenon is predicted, namely an atom-dimer scattering resonance at the location at which an Efimov state intersects the atom-dimer threshold [81, 82]. Resonance enhancement of  $\beta$  has been observed in a mixture of Cs atoms and  $\text{Cs}_2$  halo dimers [78]; see Fig. 15. The asymmetric shape of the resonance can be explained by the background scattering behavior, which here is a linear increase as function of  $a$ .

Efimov physics impacts not only the scattering properties of three identical bosons, but any three-body system in which at least two of the three pair-wise two-body interactions are large. Interestingly, depending on the mass ratio of the different components and the particle statistics, the scaling factor

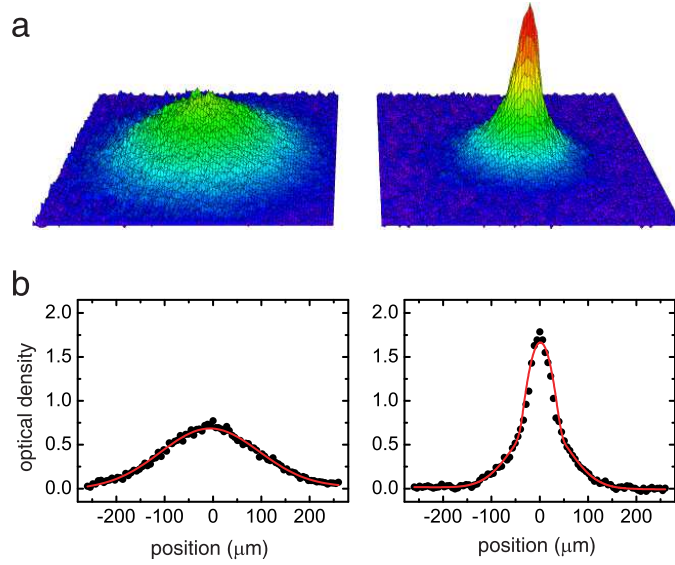


FIG. 16: Emergence of a molecular BEC in an ultracold Fermi gas of  $^{40}\text{K}$  atoms, observed in time-of-flight absorption images. The density distribution on the left-hand side (upper graph, 2D surface plot; lower graph, 1D cross section) was taken for a Fermi gas which was cooled down to 19% of the Fermi temperature. After ramping across the Feshbach resonance no mBEC was observed as the sample was too hot. The density distribution on the right-hand side was observed for a colder sample at 6% of the Fermi temperature. Here the ramp across the Feshbach resonance resulted in a bimodal distribution, revealing the presence of an mBEC with a condensate fraction of 12%. Reprinted by permission from Macmillan Publishers Ltd: Nature (London), Greiner *et al.* [35], copyright 2003.

$e^{\pi/s_0}$  can be much smaller than 22.7, facilitating the observation of successive Efimov resonances in future experiments [83].

#### D. Molecular BEC

The achievement of Bose-Einstein condensations of molecules in out of degenerate atomic Fermi gases is arguably one of the most remarkable results in the field of ultracold quantum gases. The experimental realization was demonstrated in ultracold Fermi gases of  $^6\text{Li}$  and  $^{40}\text{K}$  and turned out to be an excellent starting point to investigate the so-called BEC-BCS crossover and the properties of strongly interacting Fermi gases [18, 20]. The realization of an mBEC of Feshbach molecules is only possible in the halo regime, where the collisional properties are favorable; see Sec. IV B.

In a spin mixture of  $^6\text{Li}$ , containing the lowest two hyperfine states, the route to mBEC is particularly simple [36]. Evaporative cooling towards BEC can be performed in an optical dipole trap at a constant magnetic field in the halo region near the Feshbach resonance. In the initial stage of evaporative cooling the gas is purely atomic and molecules are produced via three-body recombination; see Sec. II B. With decreasing temperature the atom-molecule equilibrium favors the formation of molecules and a purely molecular sample is cooled down to BEC. The large atom-dimer and dimer-dimer scattering lengths along with strongly suppressed relaxation loss facilitate an efficient evaporation process. In this way, mBECs are achieved with a condensate fraction exceeding 90%.

The experiments in  $^{40}\text{K}$  followed a different approach to achieve mBEC [35]. For  $^{40}\text{K}$  the halo dimers are less stable because of less favorable short-range three-body interaction properties. Therefore the sample is first cooled above the Feshbach resonance, where  $a$  is large and negative, to achieve a deeply degenerate atomic Fermi gas. A sweep across the Feshbach resonance then converts the sample into a

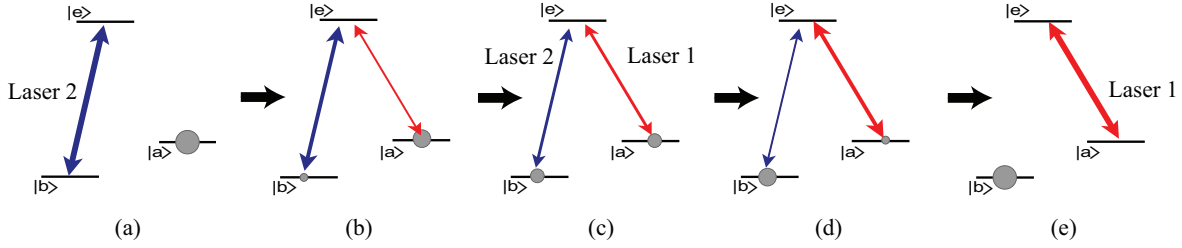


FIG. 17: Illustration of the basic idea of STIRAP. Transfer from state  $|a\rangle$  to state  $|b\rangle$ , keeping the population always in a dark state (see Eq. 8). Initially  $\Omega_2 = 1$  and  $\Omega_1 = 0$ , and finally  $\Omega_2 = 0$  and  $\Omega_1 = 1$ .

partially condensed cloud of molecules. The emergence of the mBEC in  $^{40}\text{K}$  is shown in Fig. 16.

For very large  $a$  the size of the halo dimers becomes comparable to the interparticle spacing, and the properties of the fermion pairs start to be determined by many-body physics. For  $a < 0$  two-body physics no longer supports the weakly bound molecular state and pairing is entirely a many-body effect. In particular, in the limit of weak interactions on the  $a < 0$  side of the resonance, pairing can be understood in the framework of the well-established Bardeen-Cooper-Schrieffer (BCS) theory, developed in the 1950s to describe superconductivity. Here the fermionic pairs are called Cooper pairs. The BEC and BCS limits are smoothly connected by a crossover regime where the gas is strongly interacting. This BEC-BCS crossover has attracted considerable attention in many-body quantum physics [18, 20, 84]. A theoretical description of this challenging problem is very difficult and various approaches have been developed. With tunable Fermi gases, a unique testing ground has become available to quantitatively investigate the crossover problem.

## V. TOWARD GROUND-STATE MOLECULES

Ultracold gases of ground-state molecules hold great prospects for novel quantum systems with more complex interactions than existing in atomic quantum gases. For the experimental preparation of such molecular systems, the collisional stability is an important prerequisite. This makes rovibrational ground states the prime candidates, as vibrational relaxation is energetically suppressed.

Stable BECs of dimers may for instance serve as a starting point to synthesize mBECs of more complex constituents. A particular motivation arises from the large electric dipole moments of heteronuclear dimers; see Chapter 2. This leads to the long-range dipole-dipole interaction, which is anisotropic and can be modified by an electric field. As a result, a rich variety of phenomena can be expected, with conceptual challenges and intriguing experimental opportunities. Proposals range from the study of new quantum phases and quantum simulations of condensed-matter system (Chapter 12), to fundamental physics tests (Chapters 15 and 16) and schemes for quantum information processing (Chapter 17).

The method of STImulated Raman Adiabatic Passage (STIRAP) has attracted considerable interest as a highly efficient way to coherently transfer atom pairs or Feshbach molecules into more deeply bound state [85]. The method offers a high transfer efficiency without heating of the molecular sample, thus allowing to preserve the high phase-space density of an ultracold gas. Several groups are actively pursuing such experiments with the motivation to create quantum gases of collisionally stable ground-state molecules.

### A. Stimulated Raman adiabatic passage

The basic idea of STIRAP to transfer population between two quantum states relies on a particularly clever implementation of a coherent two-photon Raman transition, involving a dark state during the transfer. For a detailed description of its principles and an overview of early applications, the reader may refer to Ref. [86].

Let us consider a three-level system with  $|a\rangle$  and  $|b\rangle$  representing two different ground state levels, and  $|e\rangle$  being an electronically excited state, as shown in Fig. 17. Laser 1 (2) couples the state  $|a\rangle$  ( $|b\rangle$ ) to the state  $|e\rangle$  and the Rabi frequency  $\Omega_1$  ( $\Omega_2$ ) describes the corresponding coupling strength [87]. The Rabi frequency is defined as  $\mathbf{d} \cdot \mathbf{E}/\hbar$ , with  $\mathbf{E}$  being the electric-field amplitude of the laser field and  $\mathbf{d}$  the dipole matrix element. The states  $|a\rangle$  and  $|b\rangle$  are long lived, whereas the excited state  $|e\rangle$  can undergo spontaneous decay into lower states.

An essential property of such a coherently coupled three-level system is the existence of a dark state  $|D\rangle$  as an eigenstate of the system. This state generally occurs if both laser fields have the same resonance detuning with respect to the corresponding transition, i.e. if the two-photon detuning is zero. The state is *dark* in the sense that it is decoupled from the excited state  $|e\rangle$  and thus not influenced by its radiative decay. The dark state can be understood as a coherent superposition of state  $|a\rangle$  and state  $|b\rangle$ ,

$$|D\rangle = \frac{1}{\sqrt{\Omega_1^2 + \Omega_2^2}} (\Omega_2|a\rangle - \Omega_1|b\rangle), \quad (8)$$

with state  $|e\rangle$  being not involved.

The key idea of STIRAP is to slowly change  $\Omega_1$  and  $\Omega_2$  in a way that the system is always kept in a dark state. This avoids losses caused by spontaneous light scattering in the excited state  $|e\rangle$  [88]. One may intuitively expect that the transfer occurs by first applying Laser 1 and then Laser 2, as in a conventional two-photon Raman transition. STIRAP instead uses a counterintuitive laser pulse scheme, in which Laser 2 is applied first. Initially, only state  $|a\rangle$  is populated (Fig. 17a); this corresponds to the dark state  $|D\rangle$  if only Laser 2 is active. If one now slowly introduces Laser 1, the dark state  $|D\rangle$  begins to evolve into a superposition of  $|a\rangle$  and  $|b\rangle$  (Fig. 17b). By adiabatically ramping down the power of Laser 2 and ramping up the intensity of Laser 1, the character of the superposition state changes and it acquires an increasing  $|b\rangle$  admixture (Fig. 17c-d). When finally Laser 1 is on and Laser 2 is turned off, the population is completely transferred to the state  $|b\rangle$  (Fig. 17e). This adiabatic passage through the dark state  $|D\rangle$  does not involve any population in the radiatively decaying state  $|e\rangle$ . We point out that the relative phase coherence of the two laser fields is an essential requirement for STIRAP. Moreover, it is important to note that the coherent sequence can be time-reversed to achieve transfer from  $|b\rangle$  to  $|a\rangle$ .

### B. STIRAP experiments

In the experiments to create quantum gases of collisionally stable ground-state molecules, the initially populated state  $|a\rangle$  corresponds to a Feshbach molecule and  $|b\rangle$  is a deeply bound molecular state. The state  $|e\rangle$  is a carefully chosen electronically excited level, which has to fulfil two important conditions. To obtain large enough optical Rabi frequencies  $\Omega_1$  and  $\Omega_2$  the state must provide sufficiently strong coupling to both states  $|a\rangle$  and  $|b\rangle$ , demanding sufficiently strong dipole matrix elements besides the technical requirement of sufficiently intense laser fields at the particular wavelengths. Moreover, state  $|e\rangle$  needs to be well separated from other excited states, as a significant coupling to these would deteriorate the dark character of the superposition state.

Proof-of-principle experiments have been performed on homonuclear  $^{87}\text{Rb}_2$  molecules [89] and heteronuclear  $^{40}\text{K}^{87}\text{Rb}$  molecules [90], demonstrating the transfer by one or a few vibrational quanta. The

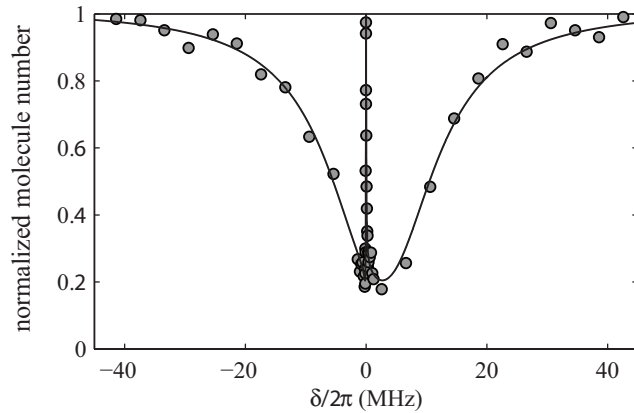


FIG. 18: Dark resonance observed as a signature of a dark state between two different vibrational levels in a trapped sample of  $^{87}\text{Rb}_2$  Feshbach molecules. Here both laser fields are turned on simultaneously, and the frequency of Laser 1 is varied while Laser 2 is kept at a fixed frequency, thus varying the two-photon detuning  $\delta$ . The population of the optically excited state  $|e\rangle$  leads to a strong background loss caused by spontaneous decay into other levels in a region corresponding to the single-photon transition linewidth. If the two-photon resonance condition is met ( $\delta = 0$ ), a suppression of loss occurs in a very narrow frequency range, which indicates the decoupling from the excited state. The behavior can be modeled on the basis of a three-state system, which provides full information on the relevant experimental parameters. In practice, the study of such a dark resonance is an important step to implement STIRAP. From Ref. [89].

STIRAP transfer of  $^{87}\text{Rb}_2$  started with trapped Feshbach molecules. In order to characterize and optimize the experimental parameters, the study of a “dark resonance” was an essential step; see Fig. 18. STIRAP could then be efficiently implemented to transfer the molecules from the last bound vibrational level ( $E_b = h \times 24$  MHz) to the second-to-last state ( $h \times 637$  MHz) with an efficiency close to 90%. In the experiment with the heteronuclear  $^{40}\text{K}^{87}\text{Rb}$  molecules, STIRAP was demonstrated with final molecular binding energies of up to  $h \times 10$  GHz.

Subsequent experiments then moved on to more deeply bound molecules and in particular to the rovibrational ground states of the triplet and the singlet potential. To bridge a large energy range with STIRAP the experiments become more challenging both for technical and for physical reasons. In particular, the optical transition matrix elements become an important issue, as they enter the optical Rabi frequencies. In molecular physics, the Franck-Condon principle states that an optical transition does not change the internuclear separation. As a consequence, the overlap of the wavefunctions between ground state and excited state, quantified by the so-called Franck-Condon factors, crucially enters into the matrix elements. A general rule of thumb can be given for finding a large Franck-Condon overlap based on a simple classical argument. The dominant part of the wavefunction occurs near the turning points of the classical oscillatory motion in a specific molecular potential. A large Franck-Condon factor for an optical transition can be expected if the classical turning points approximately coincide for the ground and excited state.

Molecules with large binding energies of about  $h \times 32$  THz were demonstrated in an experiment on  $^{133}\text{Cs}_2$  [91]. The experiment starts with the creation of a pure sample of Feshbach molecules in a weakly bound state  $|a\rangle$  with a binding energy of  $h \times 5$  MHz. Here the standard methods for association and purification are applied as described in Sec. II. A suitable Franck-Condon overlap was experimentally found for the particular choice of  $|e\rangle$  that is depicted in Fig. 19(a). The vertical arrows indicate the optical transitions at internuclear separations where maximum wavefunction overlap occurs. The applied timing sequence is shown in Fig. 19(b). In a first STIRAP pulse sequence, the molecules are transferred from  $|a\rangle$  to  $|b\rangle$  within  $15 \mu\text{s}$ . After a variable holding time in state  $|b\rangle$ , the deeply bound molecules are reconverted



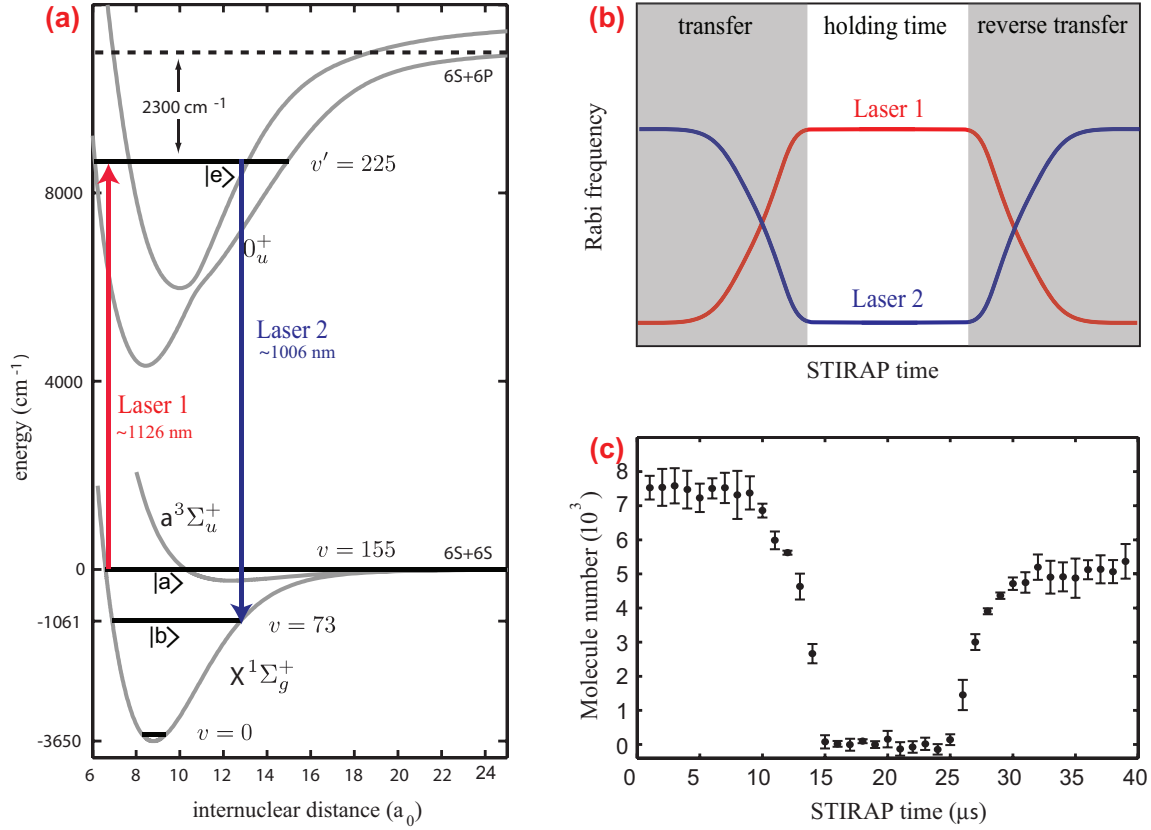


FIG. 19: STIRAP experiment starting with ultracold  $^{133}\text{Cs}_2$  Feshbach molecules. In (a) the relevant molecular potential curves and energy levels are schematically shown. The vertical arrows show the optical transitions and their positions indicate the internuclear distances where maximum Franck-Condon overlap is expected near the classical turning points. The variation of the Rabi frequencies during the pulse sequence is illustrated in (b). The experimental results in (c) show the measured molecule population in  $|a\rangle$  as a function of time through a double-STIRAP sequence. Adapted from Ref. [91].

into Feshbach molecules by a time-reversed STIRAP pulse sequence. The Feshbach molecules are then detected by the usual dissociative imaging. The experimental results in Fig. 19(c) show that 65% of the initial number of molecules reappear after the full double-STIRAP sequence, pointing to a single STIRAP efficiency of about 80%.

In the final stage of preparation of the present manuscript, breakthroughs have been achieved on the creation of rovibrational ground-state molecules in three different experiments. While Ref. [92] reports on polar  $^{40}\text{K}^{87}\text{Rb}$  molecules in both the ground state of the triplet potential ( $E_b = h \times 7.2 \text{ THz}$ ) and the one of the singlet potential ( $h \times 125 \text{ THz}$ ), Ref. [93] demonstrates homonuclear  $^{87}\text{Rb}_2$  molecules in the rovibrational ground state of the triplet potential ( $h \times 7.0 \text{ THz}$ ). A further experiment [94] has succeeded in the production of  $^{133}\text{Cs}_2$  molecules in the rovibrational ground state of the singlet potential ( $h \times 109 \text{ THz}$ ).

The successful  $^{40}\text{K}^{87}\text{Rb}$  experiment also provides a further remarkable demonstration of the importance of the Franck-Condon overlap arguments. At first glance, it may be surprising that the huge binding energy difference to the singlet ground state could be bridged in a single STIRAP step. However, an excited molecular state  $|e\rangle$  could be found for which the outer classical turning point provides good overlap with the Feshbach molecular state, while the internuclear distance at the inner turning point matches the rovibrational ground state. In the absence of such a fortunate coincidence, transfer

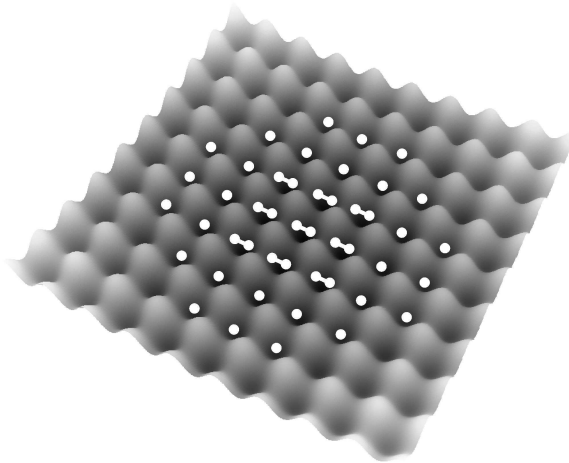


FIG. 20: Illustration of a quantum state with one molecule at each site of an optical lattice. In the central region of the three-dimensional lattice one finds exactly one molecule per site, trapped in the vibrational ground state. Such a state was prepared with  $^{87}\text{Rb}_2$  Feshbach molecules. Adapted by permission from Macmillan Publishers Ltd: Nature Phys. (London), Volz *et al.* [54], copyright 2006.

may not be feasible in a single STIRAP sequence. Two consecutive STIRAP steps involving different excited states [85, 94] promise a general way to achieve efficient ground-state transfer for any homo- or heteronuclear Feshbach molecule.

## VI. FURTHER DEVELOPMENTS AND CONCLUDING REMARKS

In the rapidly developing field of cold molecules, Feshbach molecules play a particular role as the link to research on ultracold quantum matter. In this Chapter, we have presented the basic experimental techniques and discussed some major developments in the field. In this final Section, we briefly point to some other recent developments not discussed so far, adding further interesting aspects to our overview of the research field.

Intriguing connections to condensed-matter physics can be found when Feshbach molecules are trapped in optical lattices. In this spatially periodic environment, a Feshbach molecule can be used both as a well-controllable source of correlated atom pairs, and as an efficient tool to detect such pairs. A recent experiment [95] shows how Feshbach molecules, prepared in a three-dimensional lattice, are converted into “repulsively bound pairs” of atoms when forcing their dissociation through a Feshbach ramp. Such atom pairs stay together and jointly hop between different sites of the lattice, because the atoms repel each other. This counterintuitive behavior is due to the fact that the band gap of the lattice does not provide any available states for taking up the interaction energy.

Another fascinating example along the lines of condensed-matter physics is a quantum state with exactly one Feshbach molecule per lattice site, as illustrated in Fig. 20. Such a state has vanishing entropy and closely resembles a Mott-insulator state [96]. It offers an excellent starting point for experiments on strongly correlated many-body states (Chapter 12) and on quantum information processing (Chapter 17), and for the production of a BEC of molecules in the internal ground state [85]. In the latter case, the basic idea is to convert the collisionally unstable Feshbach molecules into collisionally stable molecules in the rovibrational ground state. Then the lattice is no longer needed for isolating the molecules from each other and dynamical melting of the ordered state by ramping down the lattice may eventually lead to mBEC.

Novel phenomena can also be observed with Feshbach molecules in low-dimensional trapping schemes,

such as one-dimensional tubes realized in two-dimensional optical lattices. Here a two-body bound state can exist also for negative scattering lengths, contrary to the situation in free space [97]. Low-dimensional traps also offer very interesting environments to create strongly correlated many-body regimes. Counterintuitively, the sensitivity of Feshbach molecules to inelastic decay can inhibit loss and lead to a stable correlated state, as recently demonstrated with  $^{87}\text{Rb}_2$  in a one-dimensional trap [98].

Various mixtures of ultracold atomic species offer a wide playground for ultracold heteronuclear molecules, and the basic interaction properties of many different combinations involving bosonic and fermionic atoms are currently being explored. A new twist to the field is given by ultracold Fermi-Fermi systems, which have recently been realized in mixtures of  $^6\text{Li}$  and  $^{40}\text{K}$  [99, 100]. Molecule formation in such systems will lead to bosonic molecules, which in the many-body context may lead to new types of pair-correlated states and novel types of strongly interacting fermionic superfluids.

Another interesting question is whether more complex ultracold molecules can be created than simple dimers. A first step into this direction is the observation of scattering resonances between ultracold dimers [101] which have been found in the collisional decay of an optically trapped sample of  $^{133}\text{Cs}_2$  molecules and interpreted as a result of a resonant coupling to tetramer states.

All the examples presented in this Chapter highlight how great progress is currently being made to fully control the internal and external degrees of freedom of various types of ultracold molecules under conditions near quantum degeneracy. This will soon enable many new applications, ranging from high-precision measurements and quantum computation to the exploration of few-body physics and novel correlated many-body quantum states. Several major research themes are obvious and will undoubtedly lead to great success, but we are also confident that the field also holds the potential for many surprises and developments which we can hardly imagine now.

### Acknowledgments

We would like to thank all members of the Innsbruck group “Ultracold Atoms and Quantum Gases” ([www.ultracold.at](http://www.ultracold.at)) for contributing to our research program on Feshbach molecules. In particular, we would like to thank Johannes Hecker Denschlag and Hanns-Christoph Nägerl for the long-standing collaboration on this topic. We are also indebted to Cheng Chin, Paul Julienne, and Eite Tiesinga for the many insights gained when jointly preparing a review article on Feshbach resonances together with one of us (R.G.). We are grateful to the Austrian Science Fund (FWF) for supporting our various projects related to ultracold molecules. F.F. is a Lise-Meitner fellow of the FWF, and S.K. is supported by the European Commission with a Marie Curie Intra-European Fellowship.

- 
- [1] S. Chu, “Nobel Lecture: The manipulation of neutral particles”, *Rev. Mod. Phys.* **70**, 685 (1998).
  - [2] C. N. Cohen-Tannoudji, “Nobel Lecture: Manipulating atoms with photons”, *Rev. Mod. Phys.* **70**, 707 (1998).
  - [3] W. D. Phillips, “Nobel Lecture: Laser cooling and trapping of neutral atoms”, *Rev. Mod. Phys.* **70**, 721 (1998).
  - [4] E. A. Cornell and C. E. Wieman, “Nobel Lecture: Bose-Einstein condensation in a dilute gas, the first 70 years and some recent experiments”, *Rev. Mod. Phys.* **74**, 875 (2002).
  - [5] W. Ketterle, “Nobel lecture: When atoms behave as waves: Bose-Einstein condensation and the atom laser”, *Rev. Mod. Phys.* **74**, 1131 (2002).
  - [6] E. Arimondo, W. D. Phillips, and F. Strumia, eds., *Laser Manipulation of Atoms and Ions* (North Holland, Amsterdam, 1992), Proceedings of the International School of Physics “Enrico Fermi”, Course CXVIII, Varenna, 9-19 July 1991.

- [7] H. J. Metcalf and P. van der Straten, *Laser Cooling and Trapping* (Springer, New York, 1999).
- [8] S. Bize, P. Laurent, M. Abgrall, H. Marion, I. Maksimovic, L. Cacciapuoti, J. Grünert, C. Vian, F. Pereira dos Santos, P. Rosenbusch, P. Lemonde, G. Santarelli, P. Wolf, A. Clairon, A. Luiten, M. Tobar, and C. Salomon, “Cold atom clocks and applications”, *J. Phys. B* **38**, S449 (2005).
- [9] L. Hollberg, C. Oates, G. Wilpers, C. Hoyt, Z. Barber, S. Diddams, W. Oskay, and J. Bergquist, “Optical frequency/wavelength references”, *J. Phys. B* **38**, S469 (2005).
- [10] W. Ketterle and N. J. van Druten, “Evaporative cooling of trapped atoms”, *Adv. At. Mol. Opt. Phys.* **96**, 181 (1997).
- [11] M. H. Anderson, J. R. Ensher, M. R. Matthews, C. E. Wieman, and E. A. Cornell, “Observation of Bose-Einstein condensation in dilute atomic vapor”, *Science* **269**, 198 (1995).
- [12] C. C. Bradley, C. A. Sackett, J. J. Tollett, and R. G. Hulet, “Evidence of Bose-Einstein condensation in an atomic gas with attractive interactions”, *Phys. Rev. Lett.* **75**, 1687 (1995).
- [13] K. B. Davis, M. O. Mewes, M. R. Andrews, N. J. van Druten, D. S. Durfee, D. M. Kurn, and W. Ketterle, “Bose-Einstein condensation in a gas of sodium atoms”, *Phys. Rev. Lett.* **75**, 3969 (1995).
- [14] B. DeMarco and D. S. Jin, “Onset of Fermi degeneracy in a trapped atomic gas”, *Science* **285**, 1703 (1999).
- [15] F. Schreck, L. Khaykovich, K. L. Corwin, G. Ferrari, T. Bourdel, J. Cubizolles, and C. Salomon, “Quasipure Bose-Einstein condensate immersed in a Fermi sea”, *Phys. Rev. Lett.* **87**, 080403 (2001).
- [16] A. G. Truscott, K. E. Strecker, W. I. McAlexander, G. B. Partridge, and R. G. Hulet, “Observation of Fermi pressure in a gas of trapped atoms”, *Science* **291**, 2570 (2001).
- [17] M. Inguscio, S. Stringari, and C. E. Wieman, eds., *Bose-Einstein Condensation in Atomic Gases* (IOS Press, Amsterdam, 1999), Proceedings of the International School of Physics “Enrico Fermi”, Course CXL, Varenna, 7-17 July 1998.
- [18] M. Inguscio, W. Ketterle, and C. Salomon, eds., *Ultracold Fermi Gases* (IOS Press, Amsterdam, 2008), Proceedings of the International School of Physics “Enrico Fermi”, Course CLXIV, Varenna, 20-30 June 2006.
- [19] F. Dalfovo, S. Giorgini, L. P. Pitaevskii, and S. Stringari, “Theory of Bose-Einstein condensation in trapped gases”, *Rev. Mod. Phys.* **71**, 463 (1999).
- [20] S. Giorgini, L. P. Pitaevskii, and S. Stringari, “Theory of ultracold Fermi gases”, preprint available at <http://arxiv.org/abs/0706.3360>.
- [21] S. Stringari and L. Pitaevskii, *Bose-Einstein condensation* (Oxford University Press, London, 2003).
- [22] C. J. Pethick and H. Smith, *Bose-Einstein condensation in dilute gases* (Cambridge University Press, 2008).
- [23] R. Grimm, M. Weidemüller, and Yu. B. Ovchinnikov, “Optical dipole traps for neutral atoms”, *Adv. At. Mol. Opt. Phys.* **42**, 95 (2000).
- [24] I. Bloch, “Ultracold quantum gases in optical lattices”, *Nature Phys.* **1**, 23 (2005).
- [25] M. Greiner and S. Fölling, “Condensed-matter physics: Optical lattices”, *Nature* **453**, 736 (2008).
- [26] E. A. Donley, N. R. Clausen, S. T. Thompson, and C. E. Wieman, “Atom-molecule coherence in a Bose-Einstein condensate”, *Nature* **417**, 529 (2002).
- [27] J. Herbig, T. Kraemer, M. Mark, T. Weber, C. Chin, H.-C. Nägerl, and R. Grimm, “Preparation of a pure molecular quantum gas”, *Science* **301**, 1510 (2003).
- [28] S. Dürr, T. Volz, A. Marte, and G. Rempe, “Observation of molecules produced from a Bose-Einstein condensate”, *Phys. Rev. Lett.* **92**, 020406 (2004).
- [29] K. Xu, T. Mukaiyama, J. R. Abo-Shaer, J. K. Chin, D. E. Miller, and W. Ketterle, “Formation of quantum-degenerate sodium molecules”, *Phys. Rev. Lett.* **91**, 210402 (2003).
- [30] C. A. Regal, C. Ticknor, J. L. Bohn, and D. S. Jin, “Creation of ultracold molecules from a Fermi gas of atoms”, *Nature* **424**, 47 (2003).
- [31] J. Cubizolles, T. Bourdel, S. J. J. M. F. Kokkelmans, G. V. Shlyapnikov, and C. Salomon, “Production of long-lived ultracold  $\text{Li}_2$  molecules from a Fermi gas”, *Phys. Rev. Lett.* **91**, 240401 (2003).
- [32] S. Jochim, M. Bartenstein, A. Altmeyer, G. Hendl, C. Chin, J. Hecker Denschlag, and R. Grimm, “Pure gas of optically trapped molecules created from fermionic atoms”, *Phys. Rev. Lett.* **91**, 240402 (2003).
- [33] K. E. Strecker, G. B. Partridge, and R. G. Hulet, “Conversion of an atomic Fermi gas to a long-lived molecular Bose gas”, *Phys. Rev. Lett.* **91**, 080406 (2003).
- [34] R. Wynar, R. S. Freeland, D. J. Han, C. Ryu, and D. J. Heinzen, “Molecules in a Bose-Einstein condensate”,

- Science **287**, 1016 (2000).
- [35] M. Greiner, C. A. Regal, and D. S. Jin, “Emergence of a molecular Bose-Einstein condensate from a Fermi gas”, Nature **426**, 537 (2003).
  - [36] S. Jochim, M. Bartenstein, A. Altmeyer, G. Hendl, S. Riedl, C. Chin, J. Hecker Denschlag, and R. Grimm, “Bose-Einstein condensation of molecules”, Science **302**, 2101 (2003).
  - [37] M. W. Zwierlein, C. A. Stan, C. H. Schunck, S. M. F. Raupach, S. Gupta, Z. Hadzibabic, and W. Ketterle, “Observation of Bose-Einstein condensation of molecules”, Phys. Rev. Lett. **91**, 250401 (2003).
  - [38] C. Ospelkaus, S. Ospelkaus, L. Humbert, P. Ernst, K. Sengstock, and K. Bongs, “Ultracold heteronuclear molecules in a 3D optical lattice”, Phys. Rev. Lett. **97**, 120402 (2006).
  - [39] S. B. Papp and C. E. Wieman, “Observation of heteronuclear Feshbach molecules from a  $^{85}\text{Rb}$ - $^{87}\text{Rb}$  gas”, Phys. Rev. Lett. **97**, 180404 (2006).
  - [40] C. Weber, G. Barontini, J. Catani, G. Thalhammer, M. Inguscio, and F. Minardi, “Association of ultracold double-species bosonic molecules”, preprint available at <http://arxiv.org/abs/0808.4077>.
  - [41] T. Köhler, K. Góral, and P. S. Julienne, “Production of cold molecules via magnetically tunable Feshbach resonances”, Rev. Mod. Phys. **78**, 1311 (2006).
  - [42] C. Chin, R. Grimm, P. Julienne, and E. Tiesinga, Rev. Mod. Phys., in preparation.
  - [43] Partial waves associated with even angular momentum quantum numbers  $\ell = 0, 2, 4, 6, 8$  are by convention denoted as  $s$ ,  $d$ ,  $g$ ,  $i$  and  $l$ -waves, respectively. In the case of odd angular momentum quantum numbers  $\ell = 1, 3, 5, 7$  the partial waves are called  $p$ ,  $f$ ,  $h$  and  $k$ -waves, respectively. H. N. Russell, A. G. Shenstone, and L. A. Turner, “Report on notation for atomic spectra”, Phys. Rev. **33**, 900 (1929).
  - [44] D. S. Petrov, C. Salomon, and G. V. Shlyapnikov, “Weakly bound molecules of fermionic atoms”, Phys. Rev. Lett. **93**, 090404 (2004).
  - [45] F. A. van Abeelen and B. J. Verhaar, “Time-dependent Feshbach resonance scattering and anomalous decay of a Na Bose-Einstein condensate”, Phys. Rev. Lett. **83**, 1550 (1999).
  - [46] F. H. Mies, E. Tiesinga, and P. S. Julienne, “Manipulation of Feshbach resonances in ultracold atomic collisions using time-dependent magnetic fields”, Phys. Rev. A **61**, 022721 (2000).
  - [47] E. Timmermans, P. Tommasini, M. Hussein, and A. Kerman, “Feshbach resonances in atomic Bose-Einstein condensates”, Phys. Rep. **315**, 199 (1999).
  - [48] E. Hodby, S. T. Thompson, C. A. Regal, M. Greiner, A. C. Wilson, D. S. Jin, and E. A. Cornell, “Production efficiency of ultra-cold Feshbach molecules in bosonic and fermionic systems”, Phys. Rev. Lett. **94**, 120402 (2005).
  - [49] T. M. Hanna, T. Köhler, and K. Burnett, “Association of molecules using a resonantly modulated magnetic field”, Phys. Rev. A **75**, 013606 (2007).
  - [50] S. T. Thompson, E. Hodby, and C. E. Wieman, “Ultracold molecule production via a resonant oscillating magnetic field”, Phys. Rev. Lett. **95**, 190404 (2005).
  - [51] J. P. Gaebler, J. T. Stewart, J. L. Bohn, and D. S. Jin, “ $p$ -wave Feshbach molecules”, Phys. Rev. Lett. **98**, 200403 (2007).
  - [52] J. J. Zirbel, K.-K. Ni, S. Ospelkaus, J. P. D’Incao, C. E. Wieman, J. Ye, and D. S. Jin, “Collisional stability of fermionic Feshbach molecules”, Phys. Rev. Lett. **100**, 143201 (2008).
  - [53] G. Thalhammer, K. Winkler, F. Lang, S. Schmid, R. Grimm, and J. Hecker Denschlag, “Long-lived Feshbach molecules in a three-dimensional optical lattice”, Phys. Rev. Lett. **96**, 050402 (2006).
  - [54] T. Volz, N. Syassen, D. Bauer, E. Hansis, S. Dürr, and G. Rempe, “Preparation of a quantum state with one molecule at each site of an optical lattice”, Nature Phys. **2**, 692 (2006).
  - [55] C. Chin and R. Grimm, “Thermal equilibrium and efficient evaporation of an ultracold atom-molecule mixture”, Phys. Rev. A **69**, 033612 (2004).
  - [56] S. J. J. M. F. Kokkelmans, G. V. Shlyapnikov, and C. Salomon, “Degenerate atom-molecule mixture in a cold Fermi gas”, Phys. Rev. A **69**, 031602 (2004).
  - [57] M. Mark, F. Ferlaino, S. Knoop, J. G. Danzl, T. Kraemer, C. Chin, H.-C. Nägerl, and R. Grimm, “Spectroscopy of ultracold trapped cesium Feshbach molecules”, Phys. Rev. A **76**, 042514 (2007).
  - [58] T. Volz, S. Dürr, N. Syassen, G. Rempe, E. van Kempen, and S. Kokkelmans, “Feshbach spectroscopy of a shape resonance”, Phys. Rev. A **72**, 010704(R) (2005).
  - [59] T. Mukaiyama, J. R. Abo-Shaer, K. Xu, J. K. Chin, and W. Ketterle, “Dissociation and decay of ultracold

- sodium molecules”, *Phys. Rev. Lett.* **92**, 180402 (2004).
- [60] M. Mark, T. Kraemer, P. Waldburger, J. Herbig, C. Chin, H.-C. Nägerl, and R. Grimm, “Stückelberg interferometry with ultracold molecules”, *Phys. Rev. Lett.* **99**, 113201 (2007).
  - [61] S. Knoop, M. Mark, F. Ferlaino, J. G. Danzl, T. Kraemer, H.-C. Nägerl, and R. Grimm, “Metastable Feshbach molecules in high rotational states”, *Phys. Rev. Lett.* **100**, 083002 (2008).
  - [62] M. Bartenstein, A. Altmeyer, S. Riedl, S. Jochim, C. Chin, J. Hecker Denschlag, and R. Grimm, “Crossover from a molecular Bose-Einstein condensate to a degenerate Fermi gas”, *Phys. Rev. Lett.* **92**, 120401 (2004).
  - [63] J. J. Zirbel, K.-K. Ni, S. Ospelkaus, T. L. Nicholson, M. L. Olsen, C. E. Wieman, J. Ye, D. S. Jin, and P. S. Julienne, “Heteronuclear molecules in an optical dipole trap”, *Phys. Rev. A* **78**, 013416 (2008).
  - [64] F. Lang, P. van der Straten, B. Brandstätter, G. Thalhammer, K. Winkler, P. S. Julienne, R. Grimm, and J. Hecker Denschlag, “Cruising through molecular bound-state manifolds with radiofrequency”, *Nature Phys.* **4**, 223 (2008).
  - [65] R. J. Le Roy, *LEVEL 8.0: A Computer Program for Solving the Radial Schrodinger Equation for Bound and Quasibound Levels* (University of Waterloo Chemical Physics Research Report CP-663, 2007), see <http://leroy.uwaterloo.ca/programs/>.
  - [66] E. Braaten and H.-W. Hammer, “Universality in few-body systems with large scattering length”, *Phys. Rep.* **428**, 259 (2006).
  - [67] A. S. Jensen, K. Riisager, D. V. Fedorov, and E. Garrido, “Structure and reactions of quantum halos”, *Rev. Mod. Phys.* **76**, 215 (2004).
  - [68] S. T. Thompson, E. Hodby, and C. E. Wieman, “Spontaneous dissociation of  $^{85}\text{Rb}$  Feshbach molecules”, *Phys. Rev. Lett.* **94**, 020401 (2005).
  - [69] T. Köhler, E. Tiesinga, and P. S. Julienne, “Spontaneous dissociation of long-range Feshbach molecules”, *Phys. Rev. Lett.* **94**, 020402 (2005).
  - [70] E. Braaten and H.-W. Hammer, “Enhanced dimer relaxation in an atomic and molecular Bose-Einstein condensate”, *Phys. Rev. A* **70**, 042706 (2004).
  - [71] J. P. D’Incao and B. D. Esry, “Scattering length scaling laws for ultracold three-body collisions”, *Phys. Rev. Lett.* **94**, 213201 (2005).
  - [72] J. P. D’Incao and B. D. Esry, “Suppression of molecular decay in ultracold gases without Fermi statistics”, *Phys. Rev. Lett.* **100**, 163201 (2008).
  - [73] F. Ferlaino, S. Knoop, M. Mark, M. Berninger, H. Schöbel, H.-C. Nägerl, and R. Grimm, “Collisions between tunable halo dimers: exploring an elementary four-body process with identical bosons”, *Phys. Rev. Lett.* **101**, 023201 (2008).
  - [74] G. V. Skorniakov and K. A. Ter-Martirosian, “Three-body problem for short range forces I. Scattering of low-energy neutrons by deuterons”, *Sov. Phys. JETP* **4**, 648 (1957).
  - [75] V. Efimov, “Energy levels arising from resonant two-body forces in a three-body system”, *Phys. Lett. B* **33**, 563 (1970).
  - [76] V. Efimov, “Weakly-bound states of three resonantly-interacting particles”, *Sov. J. Nucl. Phys.* **12**, 589 (1971).
  - [77] T. Kraemer, M. Mark, P. Waldburger, J. G. Danzl, C. Chin, B. Engeser, A. D. Lange, K. Pilch, A. Jaakkola, H.-C. Nägerl, and R. Grimm, “Evidence for Efimov quantum states in an ultracold gas of caesium atoms”, *Nature* **440**, 315 (2006).
  - [78] S. Knoop, F. Ferlaino, M. Mark, M. Berninger, H. Schöbel, H.-C. Nägerl, and R. Grimm, “Observation of an Efimov-like resonance in ultracold atom-dimer scattering”, preprint available at <http://arxiv.org/abs/0807.3306>.
  - [79] E. Braaten and H.-W. Hammer, “Three-body recombination into deep bound states in a Bose gas with large scattering length”, *Phys. Rev. Lett.* **87**, 160407 (2001).
  - [80] B. D. Esry, C. H. Greene, and J. P. Burke, “Recombination of three atoms in the ultracold limit”, *Phys. Rev. Lett.* **83**, 1751 (1999).
  - [81] E. Braaten and H.-W. Hammer, “Resonant dimer relaxation in cold atoms with a large scattering length”, *Phys. Rev. A* **75**, 052710 (2007).
  - [82] E. Nielsen, H. Suno, and B. D. Esry, “Efimov resonances in atom-diatom scattering”, *Phys. Rev. A* **66**, 012705 (2002).



- [83] J. P. D’Incao and B. D. Esry, “Enhancing the observability of the Efimov effect in ultracold atomic gas mixtures”, *Phys. Rev. A* **73**, 030703 (2006).
- [84] I. Bloch, J. Dalibard, and W. Zwerger, “Many-body physics with ultracold gases”, *Rev. Mod. Phys.* **80**, 885 (2008).
- [85] D. Jaksch, V. Venturi, J. Cirac, C. Williams, and P. Zoller, “Creation of a molecular condensate by dynamically melting a Mott insulator”, *Phys. Rev. Lett.* **89**, 40402 (2002).
- [86] K. Bergmann, H. Theuer, and B. W. Shore, “Coherent population transfer among quantum states of atoms and molecules”, *Rev. Mod. Phys.* **70**, 1003 (1998).
- [87] J. R. Kuklinski, U. Gaubatz, F. T. Hioe, and K. Bergmann, “Adiabatic population transfer in a three-level system driven by delayed laser pulses”, *Phys. Rev. A* **40**, 6741 (1989).
- [88] J. Oreg, F. T. Hioe, and J. H. Eberly, “Adiabatic following in multilevel systems”, *Phys. Rev. A* **29**, 690 (1984).
- [89] K. Winkler, F. Lang, G. Thalhammer, P. v. d. Straten, R. Grimm, and J. Hecker Denschlag, “Coherent optical transfer of Feshbach molecules to a lower vibrational state”, *Phys. Rev. Lett.* **98**, 043201 (2007).
- [90] S. Ospelkaus, A. Pe’er, K.-K. Ni, J. J. Zirbel, B. Neyenhuis, S. Kotochigova, P. S. Julienne, J. Ye, and D. S. Jin, “Efficient state transfer in an ultracold dense gas of heteronuclear molecules”, *Nature Phys.* **4**, 622 (2008).
- [91] J. G. Danzl, E. Haller, M. Gustavsson, M. J. Mark, R. Hart, N. Bouloufa, O. Dulieu, H. Ritsch, and H.-C. Nägerl, “Quantum gas of deeply bound ground state molecules”, *Science* **321**, 1062 (2008).
- [92] K.-K. Ni, S. Ospelkaus, M. H. G. de Miranda, A. Pe’er, B. Neyenhuis, J. J. Zirbel, S. Kotochigova, P. S. Julienne, D. S. Jin, and J. Ye, “A high phase-space-density gas of polar molecules”, preprint available at <http://arxiv.org/abs/0808.2963>.
- [93] F. Lang, K. Winkler, C. Strauss, R. Grimm, and J. Hecker Denschlag, “Ultracold molecules in the ro-vibrational triplet ground state”, preprint available at <http://arxiv.org/abs/0809.0061>.
- [94] H.-C. Nägerl, private communication.
- [95] K. Winkler, G. Thalhammer, F. Lang, R. Grimm, J. Hecker Denschlag, A. J. Daley, A. Kantian, H. P. Büchler, and P. Zoller, “Repulsively bound atom pairs in an optical lattice”, *Nature* **441**, 853 (2006).
- [96] M. Greiner, O. Mandel, T. Esslinger, T. W. Hänsch, and I. Bloch, “Quantum phase transition from a superfluid to a Mott insulator in a gas of ultracold atoms”, *Nature* **415**, 39 (2002).
- [97] H. Moritz, T. Stöferle, K. Günter, M. Köhl, and T. Esslinger, “Confinement induced molecules in a 1D Fermi gas”, *Phys. Rev. Lett.* **94**, 210401 (2005).
- [98] N. Syassen, D. M. Bauer, M. Lettner, T. Volz, D. Dietze, J. J. Garcia-Ripoll, J. I. Cirac, G. Rempe, and S. Dürr, “Strong dissipation inhibits losses and induces correlations in cold molecular gases”, *Science* **320**, 1329 (2008).
- [99] M. Taglieber, A.-C. Voigt, T. Aoki, T. W. Hänsch, and K. Dieckmann, “Quantum degenerate two-species Fermi-Fermi mixture coexisting with a Bose-Einstein condensate”, *Phys. Rev. Lett.* **100**, 010401 (2008).
- [100] E. Wille, F. M. Spiegelhalder, G. Kerner, D. Naik, A. Trenkwalder, G. Hendl, F. Schreck, R. Grimm, T. G. Tiecke, J. T. M. Walraven, S. J. J. M. F. Kokkelmans, E. Tiesinga, and P. S. Julienne, “Exploring an ultracold Fermi-Fermi mixture: Interspecies Feshbach resonances and scattering properties of  $^6\text{Li}$  and  $^{40}\text{K}$ ”, *Phys. Rev. Lett.* **100**, 053201 (2008).
- [101] C. Chin, T. Kraemer, M. Mark, J. Herbig, P. Waldburger, H.-C. Nägerl, and R. Grimm, “Observation of Feshbach-like resonances in collisions between ultracold molecules”, *Phys. Rev. Lett.* **94**, 123201 (2005).